UNIVERSITA' DEGLI STUDI DI VERONA

DIPARTIMENTO DI FARMACOLOGIA

DOTTORATO DI RICERCA IN
BIOTECNOLOGIE APPLICATE ALLE SCIENZE BIOMEDICHE

CICLO XX

DRUG-INDUCED NEPHROTOXICITY: A MOLECULAR BIOLOGY APPROACH TO IDENTIFY EARLY MARKERS OF SEGMENT-SPECIFIC PROXIMAL TUBULE INJURY IN RAT

S.S.D. BIO/14

Coordinatore: Prof. GUIDO FUMAGALLI

Tutor: Prof. CHRISTIAN CHIAMULERA

Dottorando: Dott.ssa ARIANNA CHIUSOLO

28 Febbraio 2008

1 SUMMARY

The kidney is especially vulnerable to toxic insult by various drugs and xenobiotics because it receives nearly one quarter of the cardiac output, and transports, metabolizes and concentrates a variety of potentially toxic substances within its parenchyma As a consequence of its primary functions, the kidney is especially vulnerable to toxic insults by various drugs or xenobiotics, and thus nephrotoxicity is one of the major concerns in safety evaluation. Thus, despite the morphological complexity of the kidney, the epithelial cells of proximal tubule stand out as one of the most sensitive components in the kidney and are thus highly susceptible to damage.

Traditional markers of kidney toxicity, blood creatinine and urea, have some limitations. First, significant changes may not occur until frank renal damage has occurred (determined by histopathology assessment and/or functional tests) and second they are not region specific.

As a consequence of the difficulties in assessing renal damage by currently available/traditional biomarkers, there is an ongoing interest in developing new, early biomarkers of nephrotoxicity. Integratation of emerging transcription profiling technologies into traditional drug safety assessment evaluations offers the possibility to take new steps toward understanding mechanism of target organ toxicity and elucidating putative new biomarkers of exposure and safety.

The renal toxicity process is typically initiated by a toxic injury to tubular epithelial cells in various nephron segments and this initial injury is often followed by cellular proliferation and repair that attempts to restore normal renal function. Changes in the expression of mRNA specifically expressed in the injured kidney cells are some of the earliest events that accompany the renal injury. This is accompanied by changes in the expression of other genes that contribute either to cellular repair or recovery of renal function. In many of published literature employed microarray technology has been used to identify some patterns of gene expression that reflect different types of nephrotoxicity.

Signature of genes designed to indicate nephrotoxicity obtained need to be validated with an independent gene expression detection technology such as quantitative reverse transcriptase-polymerase chain reaction (qRT-PCR).

The objective of the present work was to evaluate potential molecular markers of proximal tubular damage in rat kidney caused by segment-specific toxic agents .

A molecular biology approach has been applied to evaluate the expression of a selected panel of four genes that are involved in different mechanisms of toxicity and can reflect different types of nephrotoxicity. The selected genes, Kidney injury molecule-1 (Kim-1), Clusterin (Cln), Osteopontin (Spp1), and Regucalcin (Rgn) are involved in different pathways, such as tissue damage, remodeling and regeneration, disruption of calcium homeostasis, oxidative stress.

Gene expression was quantified by Real-Time quantitative Polymerase Chain Reaction (qRT-PCR) in kidney samples from male rats treated with HCBD, $K_2Cr_2O_7$, and Cephaloridine, three nephrotoxicants that primarily injure specific regions of the proximal tubule via different mechanisms of action.

Conventional clinical chemistry and histopathological analysis were performed to confirm the induction of segment-specific proximal tubule damage caused by chemicals.

Results showed a correlation of gene changes with microscopic modification induced by nephrotoxicants. Moreover, the severity in proximal tubular damage evidenced in the dose-response experiments with the three compounds, were correlated with the magnitude of the transcriptional response. On the contrary, traditional clinical markers changes were observed for severe damage only, confirming the low sensitivity. Interestingly, even low severity microscopic observations were evidenced by gene expression quantification.

Moreover, since KIM-1 mRNA levels modifications were evidenced also for low dose of nephrotoxicants where no morphologic modifications were observed, it is likely to represent a potential predictive biomarker of nephrotoxicity.

In conclusion, this study confirmed that gene expression quantification may be used to detect renal tubular damage induced by nephrotoxicants. Genomic responses could represent more sensitive tool to monitor renal damage in comparison with traditional morphological and biochemical end points.

2 INTRODUCTION

2.1 Kidney

Mammalian kidneys are paired organs present in the retroperitoneum, ventrolateral and adjacent to the lumbar vertebral bodies and their corresponding transverse process. These complex organs, which function in excretion, metabolism, secretion, and regulation, are susceptible to disease insults that affect the four major anatomic structures of the kidney: the glomeruli, tubules, interstitium, and vasculature.

2.1.1 Kidney structure and function

Kidneys are organized functionally and anatomically into lobules. Each lobule represents collections of nephrons separated by the medullary rays (Fig. 1). Renal lobules should not be confused with renal lobes. Each lobe is represented by a renal pyramid. Kidneys are covered by a diffuse fibrous capsule.

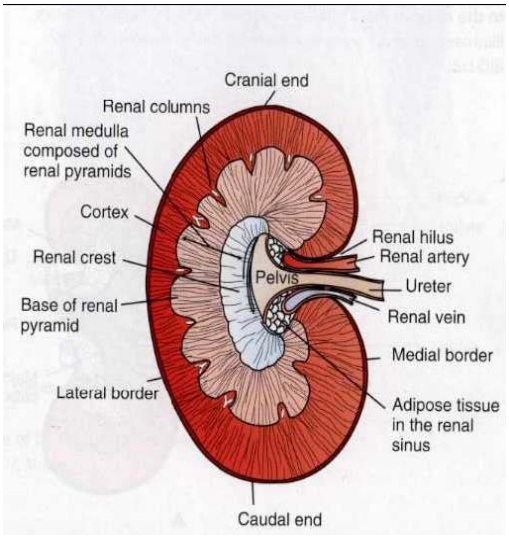

Fig. 1. Schematic diagram of kidney dorsal section (based on Illustrated Veterinary Anatomical Nomenclature, Kinderhook, NY, 1992).

The renal parenchyma is divided into a cortex and medulla. The medulla generally can be subdivided into an outer zone, that portion of the medulla close to the

cortex, and the inner zone, that portion closer to the pelvis. Papillae are surrounded by minor calyces that coalesce to form major calyces, which empty into the renal pelvis, where urine collects before entry into the ureters.

Rat kidney has a basic unipapillary architecture, the simplest type of mammalian kidney. In transverse section, the cortex and outer stripe of the outer medulla can be differentiated from the inner stripe of the outer medulla and the inner medulla with the papilla extending into the renal pelvis (Fig. 2).

The kidneys receive blood primarily through the renal artery. An interlobar artery extends along the boundary of each renal lobe (renal column) and then branches at right angles to form an arcuate artery that runs along the corticomedullary junction.

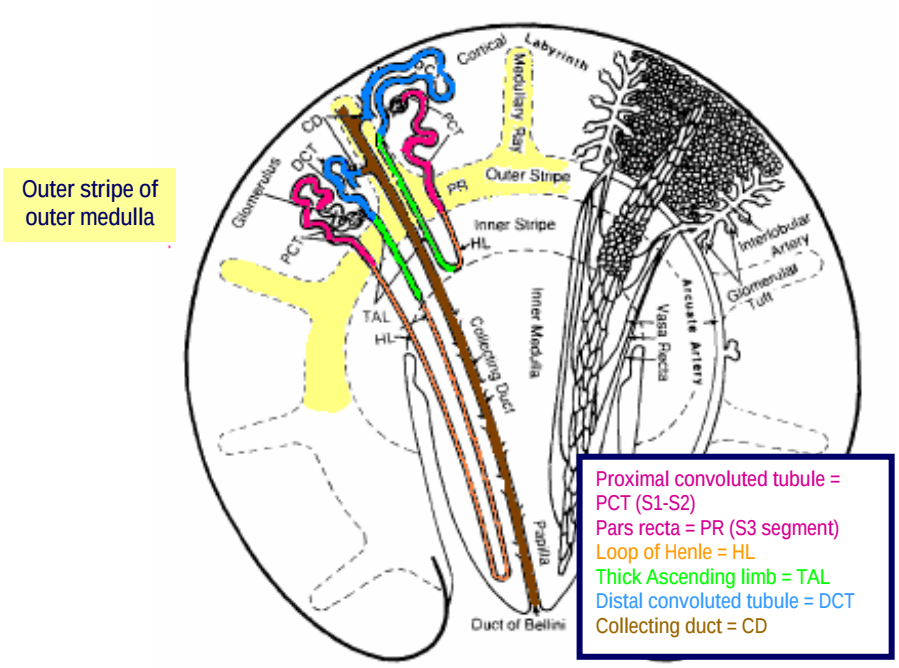

Fig. 2 Nephron topography (from Handbook of Toxicology Pathology, Academic Press, San Diego, CA)

2.1.1.1 Microscopic structure and physiology

The functional unit of the kidney is the nephron which includes the renal corpuscle (glomerulus within Bowman's capsule), and a tubular system that includes the proximal tubules, the loop of Henle and the distal convoluted tubule, which empties into the collecting tubule (Fig. 3).

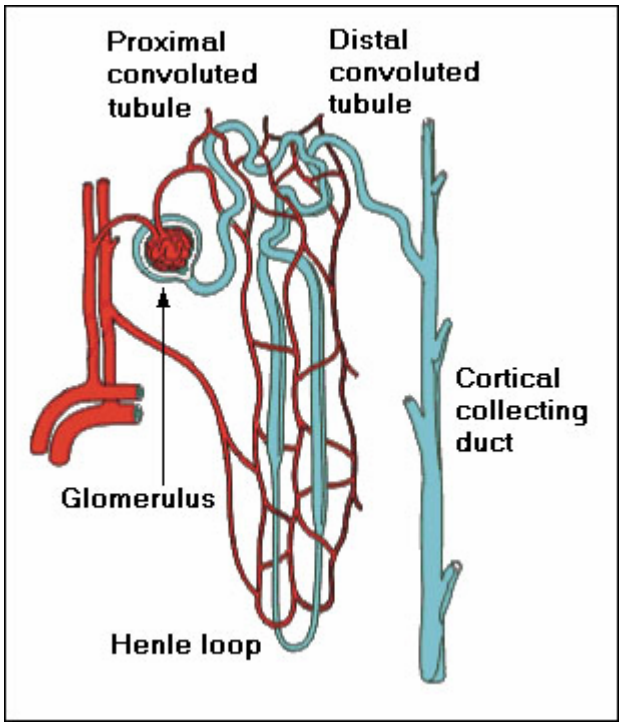

Fig. 3. Schematic diagram of the nephron (from vzajic.tripod.com/8thchapter.html).

The **glomerulus** is composed of a capillary network lined by a thin layer of endothelial cells, a central region of mesangium, and epithelial cells (podocytes). The glomerulus represents the filtering unit for blood through which the plasma filtrate is derived in the first part of the uriniferous space. The filtering membrane of the glomerulus consists of fenestrated capillary endothelial cells, a glomerular basement membrane, and visceral epithelial cells or podocytes. Discrimination in glomerular filtration for larger molecules occurs based on molecular size, configuration and charge. In addition to the principal glomerular function of plasma filtration, glomerular functions also include regulation of blood pressure by means of secreting vasopressor agents and/or hormones, regulation of peritubular blood flow, regulation of tubular metabolism, and removal of

macromolecules from circulation by the glomerular mesangium. Integral to these functions is the juxtaglomerular apparatus, which functions in tubuloglomerular feedback by autoregulating renal blood flow and glomerular filtration rate.

The **proximal tubule** is lined by columnar epithelial cells that have a microvillous (brush) border, which greatly increases their absorptive surface. A major function of the proximal tubules is to reabsorb sodium, chloride, potassium, albumin, glucose, water, and bicarbonate. This is facilitated by luminal brush border, basolateral infoldings, magnesium-dependent sodium and potassium pumps, and transport proteins. The proximal tubule begins at the urinary pole of the glomerulus and consists of an initial convoluted portion, the proximal convoluted tubule (PCT), which is a direct continuation of the parietal epithelium of Bowman's capsule and a straight portion, the pars recta, which is located in the outer stripe and/or medullary ray. The proximal tubule is divided into three segments (S1, S2, and S3) in several animal species, including rat (Fig. 2). The S1 segment is short, connecting with the glomerular filtration space. Cells of this segment have the highest rate of oxidative metabolism in the kidney. The S2 segment represents the vast majority of the PTC and extends a short distance into the pars recta. The vast majority of the pars recta consists of the S3 segment.

The transition from the proximal tubule to the thin descending limb of the **loop of Henle** is abrupt and marks the boundary between the inner stripes of the outer medulla. Four epithelial cell types are described in the thin descending and the thin ascending limbs of the loop of Henle. Ultrastructurally, they vary from non-specialized cells without interdigitation to cells with interdigitation and specialization, evidenced by a variation (increase) in the cytoplasmic number of mitochondria, and intramembranous particles, and the surface number of microvilli. The lenth of Henle's loop varies, with subcapsular nephrons having a very short loop extending only in the outer stripe. Nephrons arising in the midcortex have loops extending midway through the inner medulla. Juxtamedullary nephrons extend deep into the papilla. The transition from the pars recta to the descending loop of Henle results in a reduction in the outside diameter with only a slight change in luminal diameter. An osmotic gradient is estebilished and maintained by selective permeability in the loop of Henle (countercurrent

multipliers) and passive diffusion in the vasa recta (countercurrent exchangers). This forms the basis for a countercurrent system in which inflow runs parallel to, in intimate proximity with, and opposite to outflow. The ability of the kidneys to concentrate urine is dependent on the gradient of increasing interstitial osmolarity running from the outer medulla to the tip of the papilla created by countercurrent system (Fig. 4).

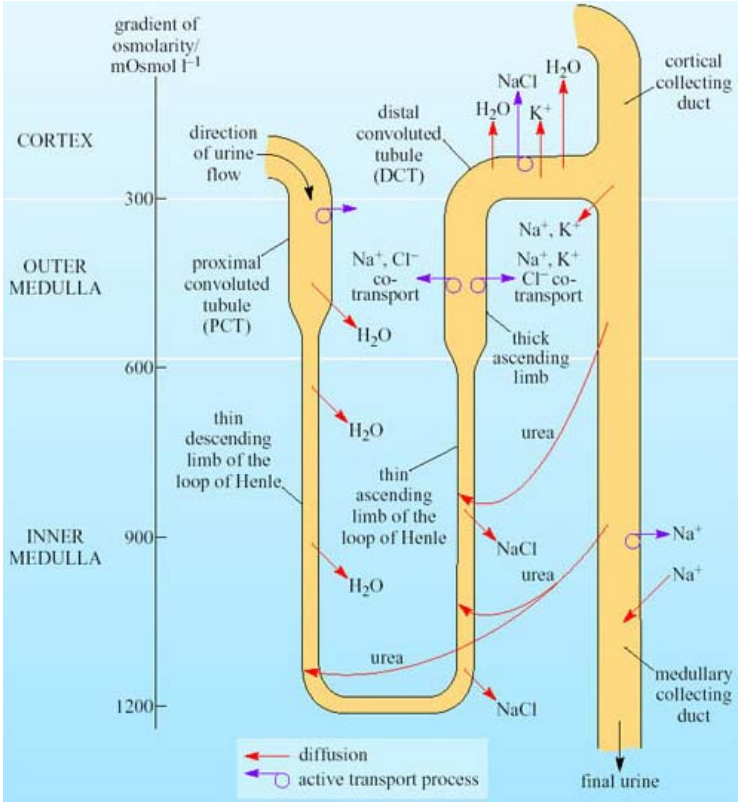

Fig. 4. Schematic diagram of the counter-current multiplier and exchanger. (From openlearn.open.ac.uk/.../2815/formats/print.htm)

The distal nephron is composed of three structurally distinct segments: the thick ascending limb of the loop of Henle, in the outer zone of the medulla and in the cortex, the macula densa, and the distal convoluted tubule. The macula densa (Fig. 5) is one of the components of the juxtaglomerular apparatus, with the renin-producing granular cells of the afferent arteriole, and the extraglomerular mesangium.

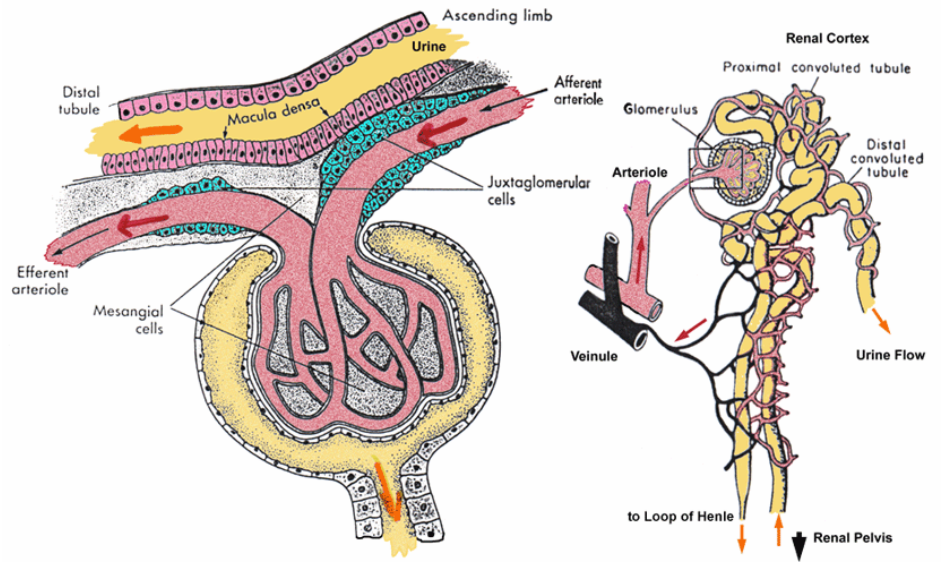

Fig. 5. Schematic diagram of the juxtaglomerular apparatus (from kcampbell.bio.umb.edu/.../Session%203.html**)**

The juxtaglomerular apparatus functions in tubuloglomerular feedback autoregulating renal blood flow and glomerular filtration rate by the renin-angiotensin-aldosterone system (Fig. 6).

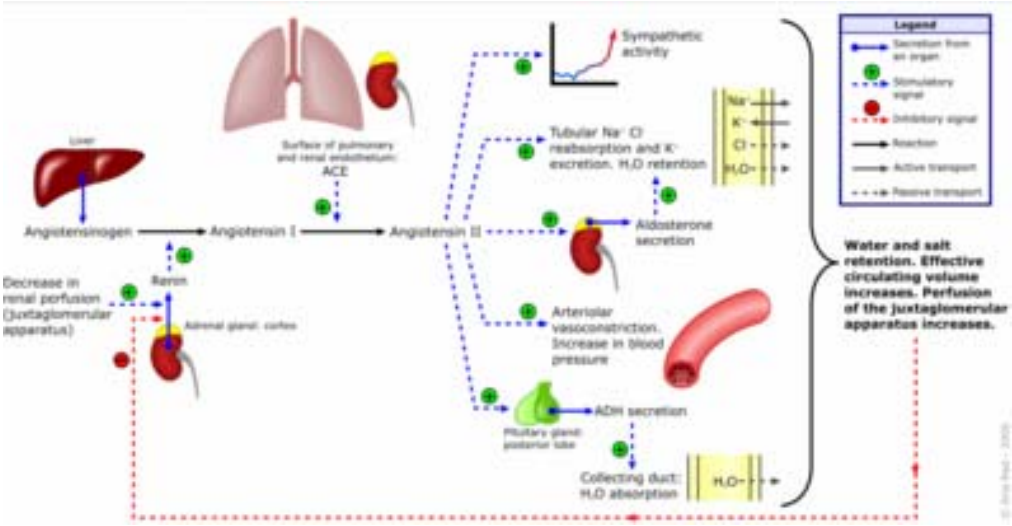

Fig. 6. Schematic diagram of the renin-angiotensin-aldosterone system

The **distal convoluted tubule** (DTC) begins at a variable distance beyond the macula densa and extends to the connecting tubule that connects the nephron with the collecting duct, which pass through the renal cortex and medulla, to empty into pelvis of the kidney at the apexes of the medullary pyramids. The epithelium

of the DTC is lower than that of the PTC. Although microvilli are present, they are not in significant numbers to form a distinctive brush border. DTC cells are involved in sodium and vasopressin stimulated water reabsorption.

2.1.1.2 Renal function

Renal function can be summarized into five basic components:

1. formation of urine for the purpose of elimination of metabolic wastes;
2. acid-base regulation, predominantly through reclamation of bicarbonate from the glomerular filtrate;
3. the conservation of water through reabsorption by the proximal convoluted tubules, the countercurrent mechanism of the loop of Henle, antidiuretic hormone activity in the distal tubules, and the urea gradient in the medulla. The tubular system is capable of absorbing up to 99% of the water in the glomerular filtrate;
4. the maintenance of normal extracellular potassium ion concentration through passive reabsorption in the proximal tubules and tubular secretion in the distal tubules under the influence of aldosterone;
5. endocrine function through three hormonal axes: renin-angiotensin, most importantly, but also erythropoietin and vitamin D. Erythtopoietin, produced in the kidneys in response to reduced oxygen tension, is released into the blood and stimulates bone marrow to produce erythrocytes. Vitamin D is converted in the kidneys to its most active form (1,25-dihydroxycholecalciferol [calcitriol]), which facilitates calcium absorption by the intestine.

2.2 Kidney toxicity

The kidney is especially vulnerable to toxic insult by various drugs and xenobiotics because it receives nearly one quarter of the cardiac output, and transports, metabolizes and concentrates a variety of potentially toxic substances within its parenchyma (Toback et al., 1992; Bennett et al., 1997).

As a consequence of its primary functions, the kidney is especially vulnerable to toxic insults by various drugs or xenobiotics, and thus nephrotoxicity is one of the major concerns in safety evaluation. Since 90% of the blood that reaches the

kidney flows through the renal cortex, it is not surprising that many xenobiotics and their metabolites affects the cells of the proximal tubules after passing the glomeruli, and since the proximal tubule reabsorbs 60-80% of solute and water, toxicant-induced injury frequently affects the water and solute balance. Thus, despite the morphological complexity of the kidney, the renal tubule epithelial cells stand out as one of the most sensitive components in the kidney and are thus highly susceptible to damage.

2.2.1 Mechanisms of toxicity

Xenobiotic-associated kidney injury typically depends on selective concentration of the toxic moiety at the target cell or subcellular organelle. This concentration is favored by normal function of the kidney. The magnitude of blood flow per gram of renal parenchyma is higher than for any other tissue. Glomerular filtration with tubular reabsorption serves to further concentrate potentially toxic moieties. Tubular transport occurs via protein binding with endocytosis, via active or passive link with ATP hydrolysis-dependent transport such as the sodium pump, or via organic anion or cation transport. Concomitantly, selective membrane permeability may serve to maintain critical concentrations of molecules concentrated via transport.

The kidney has the capacity to dissociate protein-bound toxins; such binding serves to protect other tissues from the injurious agent. The kidney also has the capability to alter the pH of tubular fluid, which can serve to transform solutes to a reactive form. Finally, the kidney partecipates in the metabolism of xenobiotics. Renal metabolism with derivation of reactive electrophilic intermediates causes injury following covalent reaction or peroxidative reaction with the target cell mecromolecules.

Classification of nephrotoxins

Nephrotoxins can be categorized according to intrinsic structural or functional characteristics of the xenobiotic (Table 1).

Naturally occuring organic toxins Afatoxin Bacterial toxins Furan derivates	*Nonsteroidal anti-inflammatories* Acetaminophen Ibuprofen Indomethacin
Miscellaneous therapeutics Interferon Cimetidine Isoniazid Iron Zinc	*Cancer therapeutics/Immunosuppressors* Cisplatin Vincristine Puromycin Nitrosourea Cyclosporin A
Metals Aluminum Arsenic Cadmium Mercuric chloride Gold Lead Lithium	*Herbicides* Bipyridium compounds Insecticides Chlorinated hydrocarbons Organophosphorous *Antibiotics* Cephaloridine Gentamicin Tetracycline Streptomycin
Glycols/Alogenated alkenes Hexachloro-1,3-butadiene	

Table 1 Listing and classification of nephrotoxins according to functional characteristics of the inducing agent (Kanwar NM et al., Handbook of Toxicology Pathology, Volume 2, Academic Press, 1991)

Xenobiotic causing kidney injury can be also classified into one of the following five mechanistic categories: (1) directly perturbing cellular or subcellular organelle function, (2) causing injury via reactive intermediates or peroxidative stress, (3) perturbing levels of cellular, interstitial, or lumen substrate, (4) perturbing renal hemodynamics, or (5) eliciting immune-mediated injury.

2.2.2 Proximal tubular toxicity

Several xenobiotic substances damage renal proximal tubule, the portion of the nephron with the greater sensitivity to nephrotoxic effects. Proximal tubular toxins frequently affect both convoluted and straight segments. These segments may be differentially affected by xenobiotics through the five basic mechanistic categories described above.

The proximal convoluted tubule (S_1 and S_2 segments) contains a very active endocytosis/lysosomal apparatus, thus representing the site of injury related to lysosomal overload, as well as protein-bound toxic moieties.
The straight portion of the proximal tubule (S_3 segment) represents the most susceptible site of injury via metabolic activation, transporter-associated accumulation, and hypoxia/reperfusion (Khan et al., 2002).
Among chemicals damaging the proximal tubule are antibacterial drugs such as cephaloridine (Silverblatt et al., 1970) and aminoglycosides (Wellwood et al., 1976), which selectively affect S_1-S_2 segments, anticancer drugs such as cis-Pt (Dobyan et al., 1980), which affects S_3 segment, industrial chemicals (metals and solvents) such as cadmium (Squibb et al., 1979) and hexavalent chromium (Biber et al., 1968; Evan and Dail, 1974), which affects S_1-S_2 segments, or mercury (Eknoyan et al., 1982; Dobyan and Bulger, 1984), hexachlorobuta-1,3-diene or HCBD (Ishmael et al., 1982), and palladium (Trevisan et al., 2002), which affect S_3 segment.

2.2.3 Histopathology findings

Renal tubular epithelial cells respond to nephrotoxicants by undergoing degeneration, necrosis or apoptosis. Degeneration is the result of a mild, potentially reversible injury. Degenerating cells are characterized histologically by pale, swollen cytoplasm, containing large, variably sized clear vacuoles (vacuolar degeneration). These features are the consequence of the nephrotoxicant-induced alteration in the intracellular electrolytes balance, leading to net influx of water, which, in turn, caused swelling of the plasma membrane and cytoplasmic organelles (mitochondria, smooth and rough endoplasmic reticulum, Golgi apparatus, lysosomes). For those cells more severely and irreversibly injured, death occurs by two mechanisms, necrosis and, less frequently, apoptosis. Necrotic cells are characterized by slightly swollen, brightly eosinophilic cytoplasm due to loss of normal basophilia imparted by RNA in the cytoplasm or to increased binding of eosin to denaturated intracytoplasmic proteins. Nuclear changes include shrinkage, fragmentation and fading (named pyknosis, karyorrhexi and karyolysis, respectively) or, with the passage of time, nuclei totally disappear. Apoptotic cells appear as round, brightly eosinophilic structures,

with condensed chromatin, individualized from the adjacent epithelial cells. Necrotic and apoptotic cells exfoliate into the lumen, leaving an intact basement membrane. Evidences of tubular epithelium regeneration, following nephrotoxicants induced injury, are represented by flattened cells with deeply basophilic cytoplasm, plump vesicular nuclei and prominent nucleoli and mitotic figures.

2.2.4 Clinical biomarkers

Traditional markers of kidney toxicity are blood urea nitrogen (BUN) and serum creatinine measurements. Urea and creatinine are nitrogenous end products of metabolism. Urea is the primary metabolite derived from dietary protein and tissue protein turnover. Creatinine is the product of muscle creatine catabolism. Both are relatively small molecules (60 and 113 daltons, respectively) that distribute throughout total body water. In Europe, the whole urea molecule is assayed, whereas in the United States only the nitrogen component of urea (the blood or serum urea nitrogen, i.e., BUN or SUN) is measured. The BUN, then, is roughly one-half of the blood urea.

The BUN and creatinine are screening tests of renal function. Because they are handled primarily by glomerular filtration with little or no renal regulation or adaptation in the course of declining renal function, they essentially reflect the glomerular filtration rate (GFR). The GFR is clinically important because it is a measurement of renal function. Unfortunately, their relation to GRF is not a straight line but rather a parabolic curve. Their values remain within the normal range until more than 50% of renal function is lost.

Thus, these traditional markers of kidney toxicity have two limitations (Duarte and Preuss, 1993). First, significant changes may not occur until frank renal damage has occurred (determined by histopathology assessment and/or functional tests) and second they are not region specific.

Also urinary enzymes are used to determine damage along the nephron and to define subcellular involvement (Price et al., 1982). The lysosomal enzyme N-acetylglucosaminidase (NAG) and the brush border enzyme γ-

glutamyltranspeptidase (GGT) have also been used to assess renal toxicity (Gibey et al., 1981; Scherberich and Mondorf, 1983). When tubules are damaged, NAG and GGT are excreted into the lumen of the tubules and can be detected in the urine. However, a limiting factor in the use of these enzymes, particularly NAG, is the considerable intra and inter-individual variation in urinary enzyme activity (Naidu and Lee, 1994). Consequently, 24-hour urine collection must be obtained to allow for diurnal variation of excretion and urine volume.

Recently, urinary levels of specific enzymes have been proposed as topographically specific markers of renal damage (Kilty et al. 1998). The proximal tubule is the portion of the nephron with greater sensitivity to nephrotoxic effects of chemicals, and it is the site of several metabolic activities.

Enzyme distribution along the proximal tubule segments is well defined for a number of these (Guder and Ross, 1984). Particularly, glutamine synthetase (GS) enzyme which is localized only in the early and late portion of the S3 segment (Burch et al., 1978). GS is a mitochondrial enzyme present in a variety of tissues including kidney (Iqbal and Ottaway, 1970). According to the S3 segment-specific localization, GS activity in urine is able to identify a damage of this segment. At the moment, GS is the only known enzyme with an exclusively segmentary localization; therefore, this enzyme may identify only whether a xenobiotic substance affects S3 segment by increase of excretion (Trevisan et al., 1999).

2.2.5 Genomic approach to nephrotoxicity

As a consequence of the difficulties in assessing renal damage by currently available/traditional biomarkers, there is an ongoing interest in developing new, early biomarkers of nephrotoxicity (Duan et al. 1999;Taylor et al., 1997).

An emerging approach to achieve this objective is the use of genomic technologies that are impacting in many areas of drug-discovery and development (Afshari et al., 1999).

Integratation of emerging transcription profiling technologies into traditional drug safety assessment evaluations offers the possibility to take new steps toward

understanding mechanism of target organ toxicity and elucidating putative new biomarkers of exposure and safety.

The renal toxicity process is typically initiated by a toxic injury to tubular epithelial cells in various nephron segments. The initial injury is often followed by cellular proliferation and repair that attempts to restore normal renal function (Toback et al., 1992). Changes in the expression of mRNA specifically expressed in the injured kidney cells are some of the earliest events that accompany the renal injury. This is accompanied by changes in the expression of other genes that contribute either to cellular repair or recovery of renal function.

Recent application of microarray-based gene profiling has provided a first insight into toxicity-related gene expression changes in the kidney (Amin et al., 2004; Thukral et al., 2005). In these works, through comparison of the expression profiles derived from kidneys exposed to different known nephrotoxicants (associated with varying types and severity of toxicity), some patterns of gene expression that reflect different types of nephrotoxicity have been identified.

The development of toxicity profiles and specific gene expression signatures requires the use of standardized conditions and the testing of a number of drugs of distinct classes and mechanisms, and therefore they are usually developed on one platform technology. Analytical validation of the veracity of gene changes within a signature is usually performed with an independent gene expression detection technology such as quantitative reverse transcriptase-polymerase chain reaction (qRT-PCR).

2.3 Objective of the thesis

The objective of the present work was to evaluate potential molecular markers of proximal tubular damage in rat kidney caused by segment-specific toxic agents .

A molecular biology approach has been applied to evaluate the expression of a selected panel of four genes that are involved in different mechanisms of toxicity and can reflect different types of nephrotoxicity.

Conventional clinical chemistry and histopathological analysis were performed to confirm the induction of segment-specific proximal tubule damage caused by chemicals.

In details, the work was structured in the following experimental steps (Scheme 1):

- Treatment of male rats with three different nephrotoxicants selective for the proximal tubule segments;
- Kidney processing through gene expression quantification by quantitative real-time polymerase chain reaction (qRT-PCR);
- Kidney histopathology evaluation;
- Blood clinical chemistry markers measurement.
- Gene expression, histopathology and blood biochemical markers data integration.

In the first part of the work, as a low-scale validation of the selected genes panel, two xenobiotic chemicals (Potassium dicromate ($K_2Cr_2O_7$) and Hexachlorobuta-1,3-diene (HCBD)) were used due to their characteristic to selectively affect the different segments of the proximal tubule.

A single toxic dose for each chemicals was used to treat rats with different ages to monitor the proximal tubule damage and to identify the most susceptible stage (ageing study). Moreover, another study was set up using three different doses of the two chemicals in rats with the same age (dose-response study).

In the second part of the work, a drug known to induce a proximal tubule segment-specific injury, cephaloridine, was tested at different doses in rats (dose-response study). Results were compared with those obtained in the low-scale validation phase.

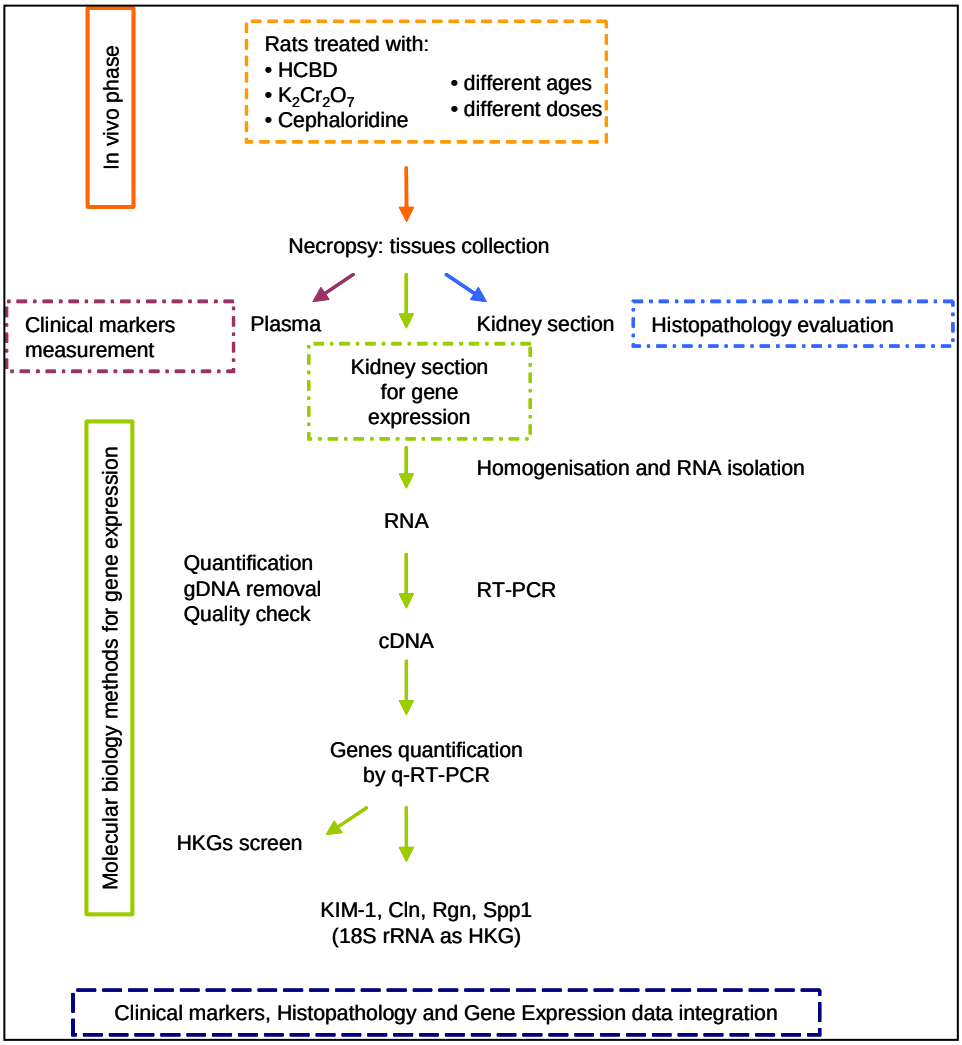

Scheme 1. Flow chart of experimental phases used in the work of thesis.

2.3.1 Genes evaluated

Kidney injury molecule-1 (Kim-1) is a type 1 transmembrane protein that is not detectable in healthy kidney tissue. Transcript levels for the gene that encodes Kim-1 are strongly upregulated in dedifferentiated proximal tubule epithelial cells in kidney after ischemic or toxic injury.

Renal epithelial cell injury is a feature of many acute and chronic renal diseases. Morphologic characteristics of injury to the proximal tubule epithelial cell include loss of proximal tubular brush border, loss of cellular polarity, dedifferentiation, and apoptosis. With advanced injury, viable and necrotic tubular epithelial cells detach from the basement membrane and contribute to intraluminal obstruction. Surviving dedifferentiated cells spread over the denuded basement membrane, undergo mitogenesis, and ultimately redifferentiate and reestablish normal epithelial polarity resulting in a normal functional epithelium (Scheridan et al., 2000; Thadhani et al., 1996). Although these processes are well described at the histopathological level, very little is known about the molecular factors that regulate these events. One of the genes identified from postischemic rat kidney by representational difference analysis (Hubank et al., 1994) was designated as KIM-1 (Ichimura et al., 1998). This gene encodes a type I cell membrane glycoprotein containing, in its extracellular portion, a six-cysteine immunoglobulin-like domain and a mucin domain. Immunoglobulin-like domains have been widely implicated in mediating protein-protein interaction (Barclay et al., 1999) in particular at the cell surface where they are responsible for cell-cell and cell-extracellular matrix interactions. The mucin domain could play a dual role of configuration and protection (Jentoft et al., 1990) as well as being involved in cell adhesion. The cytoplasmic domain of KIM-1 is relatively short and possesses a potential phosphorylation site, indicating that KIM-1 may be a signaling molecule.

Rat KIM-1 mRNA and protein levels are dramatically up-regulated in the postischemic kidney. *In situ* hybridization and immunohistochemistry revealed that KIM-1 is expressed in dedifferentiated proximal tubular epithelial cells in damaged regions, especially in the S3 segment of the proximal tubule in the outer stripe of the outer medulla, a region that is highly susceptible to injury as a result of ischemia or toxins (Ichimura et al., 1998). Because KIM-1 colocalizes with

markers of proliferation, KIM-1 has been proposed to play a role in the regeneration process.

Clusterin (Cln**)** is a heterodimeric glycoprotein and it is widely and prominently induced in injured tissue, particularly when such injury involves the kidney and the brain. While the function of clusterin in injury remain uncertain, a number of studies point to cytoprotective actions of clusterin induced in such settings.

Clusterin induces aggregation of some but not all cells *in vitro* and also is a potent cell adhesion molecule (Silkensen et al., 1999). Prolonged incubation of cells with clusterin results in the formation of junctional contacts between cells and expression of cell adhesion molecules. Clusterin may also be involved in more complex cell interactions.

Abnormalities in cell interactions occur following renal injury leading to cell rounding, retraction and detachment; decreased binding of cells to matrix components is also recognized as well as aberrant cell-cell attachments (Silkensen et al., 1995). Loss of intercellular contact may also induce apoptosis. The loss of cell-cell and cell-substratum interactions incurs detachment of tubular epithelial cells and in turn, denudation of the epithelium and tubular back leak of filtrate. Thus, even mild injury can lead to profound nephron dysfunction mediated in part through alterations in cell attachment. Loss of normal cell interactions from their usual cellular contacts and substratum lead to variable effects on cellular viability. In the setting of renal injury, promoting cell-cell contacts may enhance cell survival by allowing the exchange of critical nutrients or other factors between cells, or by providing the correct intracellular signals to prevent apoptosis. Promoting cell-substratum contacts would prevent sloughing of cells. In addition, maintenance of cell proximity would allow the normal junctional contacts to become re-established once the phase of injury subsides and the processes of repair and regeneration are initiated.

The prominent induction of clusterin in tubules following injury coupled with the capacity of this protein to promote cell interactions led to hypothesize that the induction of clusterin in states of injury provides an adaptive response that attenuates injury that otherwise occurs.

Immunohistochemistry and in situ hybridization demonstrated clusterin primarly in the inner stripe of the outer medulla (Silkensen et al., 1996).

Regucalcin (Rgn) is a Ca^{2+}-binding protein and it plays a pivotal role in maintaining intracellular calcium homeostasis by activating Ca^{2+} pump enzymes in the plasma membrane (basolateral membrane), microsomes (endoplasmic reticulum) and mitochondria of many cell types. Regucalcin has a suppressive effect on calcium signaling from the cytoplasm to the nucleus in the proliferative cells. Also, regucalcin has been demonstrated to transport to nucleus, and it can inhibit nuclear protein kinase, protein phosphatase, and deoxyribonucleic acid (DNA) and ribonucleic acid (RNA) synthesis. Regucalcin can control enhancement of cell proliferation due to hormonal stimulation (Yamaguchi et al., 2000).

The kidney plays a physiologic role in the regulation of calcium homeostasis in blood by reabsorption of urinary calcium.It has been demonstrated that regucalcin mRNA is expressed in the kidney cortex but not the medulla of rats, and that the expression may be mediated through Ca^{2+}/calmodulin action induced by calcium administration (Yamaguchi et al., 1995). This suggests a role for regucalcin in calcium metabolism of kidney cells. Presumably, regucalcin is responsible for ATP-dependent transcellular Ca^{2+} transport, and it participates in the promotion of Ca^{2+} reabsorption in the nephron tubulo of kidney cortex. Kidney regucalcin may play a physiological role in the regulation of calcium metabolism in blood through reabsorption of urinary calcium.

Osteopontin (OPN) is a phosphorylated glycoprotein that has many functions in cell-cell binding and cell-matrix binding in various organs. Osteopontin is synthesized at the highest levels in bone and epithelial tissues and is considered to play a role in bone remodelling. OPN is present in normal kidneys, has up-regulated expression and many potential roles in abnormal kidneys.

In the normal kidney, OPN shows scattered localization in distal convoluted tubules, thick ascending limbs, collecting ducts, and especially in aged rat Bowmann's capsule epithelial cells (Lopez et al., 1993). After renal damage, OPN

expression may be significantly up-regulated in all tubule segments and glomeruli.

Osteopontin is associated with a number of functions involving regulation of osteoclast function during bone formation, renal stone formation, tumorigenesis and transformation, and accumulation of macrophages (Denhardt et al., 1993). In addition, it has immune functions, inhibits induction of inducible nitric oxide synthase (iNOS), and protects cells from apoptosis as a survival factor. Recently, it has been demonstrated that OPN is associated with cell proliferation and regeneration in the recovery process after renal injury (Xie et al., 2001).

OPN has some protective actions in renal injury, such as increasing tolerance to acute ischemia, inhibiting inducible nitric oxide synthase and suppressing nitric oxide synthesis, reducing cell peroxide levels and promoting the survival of cells exposed to hypoxia, decreasing cell apoptosis and participating in the regeneration of cells. In addition, OPN is associated with renal stones, but whether it acts as a promoter or inhibitor of stone formation is controversial.

The expression of OPN is up-regulated in the injury and recovery processes of a lot of tissues and cells, including inflammation, fibrosis, mineralization and regeneration of kidneys, bone heart, vessels and cultured cells. Its expression is regulated by many factors including hormones, growth factors, cytokines, vitamin D_3, calcium, phosphate and drugs.

2.3.2 Nephrotoxicants used

Hexachlorobuta-1,3-diene (HCBD), a halogenated alkene, is a selective nephrotoxin and a nephrocarcinogen in rats, damaging selectively the pars recta of the proximal tubules (Boroushaki et al., 2003). Its organ-specific toxicity is based upon a multistep bioactivation mechanism involving hepatic and renal enzymes (Scheme 2) (Birner et al., 1997). Coniugation in Phase II metabolism with glutathione (GSH), typically decreases the reactivity of the metabolic intermediate, correspondingly reducing toxicity potential. There is now evidence however, that stable GSH conjugates , which are degraded to cysteine conjugates, may be sebsequently bioactivated to a toxic metabolite by a renal cysteine

conjugate ß-lyase (ß-lyase pathway). ß-lyase cleaves S-cysteine conjugates to putative reactive thiols. ß-lyase enzyme activity is localized mainly in the pars recta. For this reason , glutathione conjugation appears to be the only bioactivation pathway leading to reactive intermediates. These thiols are accumulated in the kidney by the organic anion transport system and is thought to be responsible for nephrotoxic effects observed in rats.

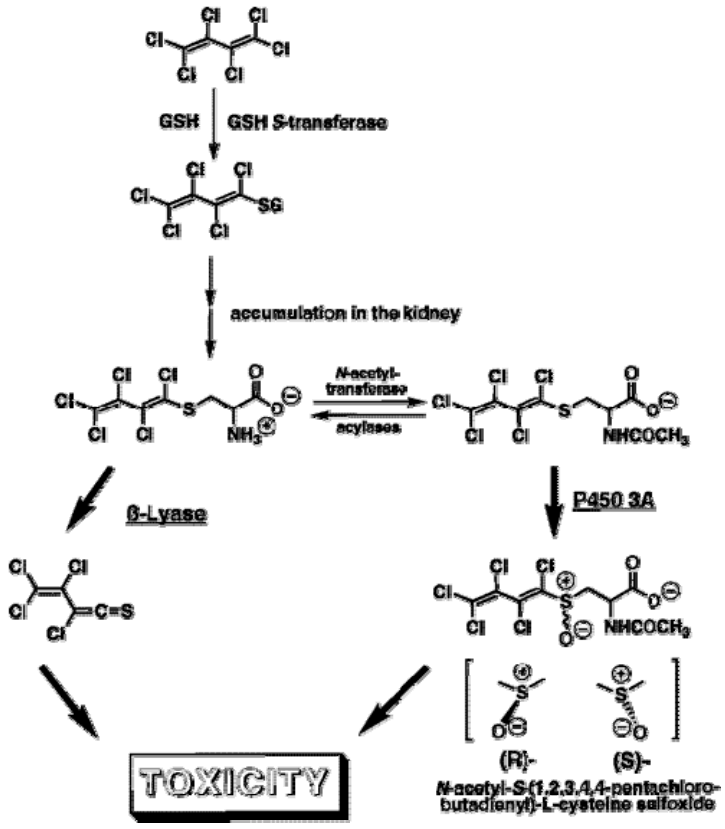

Scheme 2. Bioactivation of Hexachlorobutadiene by Glutathione Conjugation (from Birner et al., 1997)

Potassium dichromate ($K_2Cr_2O_7$) is a chemical compound widely used in industry. The oxidation state and solubility of chromium (Cr) compounds determine their toxicity. In contrast to Cr^{3+}, which is a naturally occurring form and an essential trace element for humans and others mammals, Cr^{6+} compounds are highly toxic (Wang et al., 2006). $K_2Cr_2O_7$ is a hexavalent form of Cr and has been demonstrated to induce oxidative stress and carcinogenic in nature (Stohs and Bagchi, 1995, and Bagchi et al., 2002). The kidney is the principal route of Cr excretion and it has been reported that acute exposure induces an increase in Cr

kidney content on $K_2Cr_2O_7$-treated rats (Pedraza-Chaverri et al., 2005). Exposition to Cr^{6+} produced anatomical lesions at the level of the proximal tubular cells. the first two proximal tubule segments, S1 and S2, are the primary cellular targets for Cr^{6+} toxicity. Interestingly, evidences suggest that reactive oxygen species (ROS) are involved in Cr^{6+}-induced cell injury (Stohs and Bagchi, 1995; Bagchi et al., 2002; and Travacio et al., 2001). Cr reduction intermediates, Cr^{5+} and Cr^{6+} , may be toxic as they involve ROS production (Stohs et al., 2000; Shi and Dalal, 1994) which may be generated during physiological conditions. In vitro, chromate reduction via hydrogen peroxide (H_2O_2) has been shown to produce hydroxyl radical ($OH^{\bullet}$) via a Fenton-like reaction (O´Brien and Kortenkamp, 1994; Liu et al., 1997 and Tsou et al., 1996). In vivo experiments have been shown that $K_2Cr_2O_7$ exposition induces oxidative and nitrosative stress measured as protein carbonyl content and 3-nitrotyrosine (3-NT) immunostaining (Pedraza-Chaverri et al., 2005). The role of oxidative stress in the renal damage induced by $K_2Cr_2O_7$ has been supported by the fact that some antioxidants such as α-tocopherol, ascorbic acid, and glutathione (Appenroth and Winnefeld, 1998, Arreola-Mendoza et al., 2006), and the previous induction of heme oxygenase-1 (Barrera et al., 2003a and Barrera et al., 2003b) are able to ameliorate $K_2Cr_2O_7$-induced nephrotoxicity and oxidative damage.

Cephalosporins and other ß-lactam antibiotics cause proximal tubular necrosis in human and laboratory animals. Selective toxicity to the proximal tubule occurs because of high intracellular concentration achieved by active transport by the organic anion transporter. The pars recta represents the segment of nephron with greatest injury from cephalosporins.

As a model cephalosporin, cephaloridine is metabolized in the proximal tubular cell and, at sufficiently high concentrations, induces lipid peroxidation-type injury to membranes. Evidence for oxidative stress as a mechanism of injury includes (1) inhibition of injury by superoxide dismutase, by catalase, by the hydroxyl radical scavanger mannitol and by the singlet oxygen scavenger histidine; (2) increase in malondialdehyde production in vitro; (3) superoxide anion generation in vitro; (4) gluthatione depletion of renal cortex from treated animals; and, (5) potentiation of

injury by pretreatment with antioxidant-deficient diets (vitamin E and selenium). The importance of metabolism and the generation of reactive intermediates are indicated by the demonstration of covalent binding of the renal cortex homogenate microsomal fraction by cephalosporins in a quantity proportional to their toxic potential.

2.3.3 Polymerase Chain Reaction (PCR) and Reverse Transcription Polymerase Chain Reaction (RT-PCR)

The advent of Polymerase Chain Reaction (PCR) by Kary B. Mullis in the mid-1980s revolutionized molecular biology as we know it. PCR is a fairly standard procedure now, and its use is extremely wide-ranging. At its most basic application, PCR can amplify a small amount of template DNA (or RNA) into large quantities in a few hours. Typical reasons for amplifying particular gene sequences are to determine the presence or absence of the sequence, for expample DNA of infectious agents, such as mycobacteria (Perosio and Frank, 1993) or chromosome translocation (Lee et al., 1987), to determine whether a mutational hotspot contains a disease-related mutation or to study clonality of rearranged antigen receptor genes in lymphocyte populations (Diss and Pan, 1997).

PCR reaction is performed by mixing the DNA with oligonucleotide primers, complementary to a defined sequence on each of the two strands of the DNA, on either side of the DNA (forward and reverse), Taq polymerase (of the species Thermus aquaticus, a thermophile whose polymerase is able to withstand extremely high temperatures), free nucleotide triphosphates (dNTPs for DNA, NTPs for RNA), and appropriate buffer solution. The temperature is then alternated between hot and cold to denature and reanneal the DNA, with the polymerase adding new complementary strands each time.

In details, the reaction is first heated to 95^{o}C to melt (denature) the double strand DNA into separate starnds. The reaction is then cooled to ~50^{o}C, at which temperature the primers will find base-complementary regions in the single strand DNA, to which they will stick (anneal). The reaction is finally heated to 72^{o}C, at which temperature the *Taq* enzyme replicates the primed single strand DNA

(extension). At the end of one cycle, the region between the two primers has been copied once, producing two copies of the original gene region (Fig. 7).

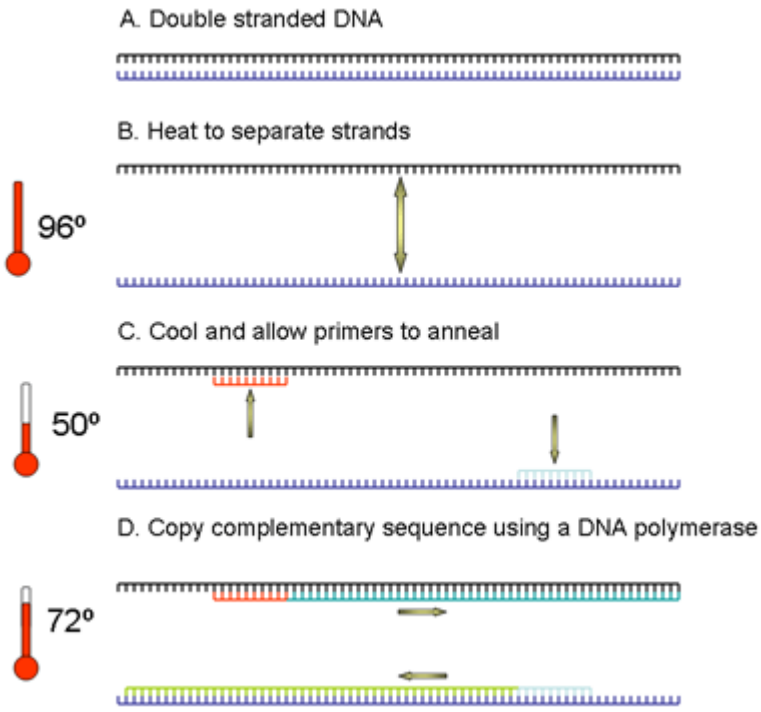

Fig.7. Stepwise representation of PCR (from pathmicro.med.sc.edu/pcr/realtime-home.htm)

Because a heat-resistant polymerase is used, the reaction can be repeated continuously without addition of more enzyme. Each cycle *doubles* the copy number of the amplified gene: ten cycles produces 2 → 4 → 8 → 16 → 32 → 64 → 128 → 256 → 512 → 1,024 (2^{10}) copies. Thus, 30 cycles yields a (2^{10x3}) = 10^9-fold amplification. This produces a sufficient quantity of the gene region of interest for direct analysis, for example by DNA sequencing. After several (often about 40) rounds of amplification, the PCR product is analyzed by agarose or polyacriylamide gel electrophoresis followed by ethidium bromide staining and viewing under UV illumination. The choise depends on the product size and resolution required. For larger products (300bp and larger) agarose gels are more convenient and use less toxic reagents. If smaller fragments must be accurately sized, then polyacrylamide gels are required

This method of analysis is at best semi-quantitative and, in many cases, the amount of product is not related to the amount of input DNA making this type of PCR a qualitative tool for detecting the presence or absence of a particular DNA.
In order to measure messenger RNA (mRNA), the method was extended using reverse transcriptase enzyme to convert mRNA into complementary DNA (cDNA) which was then amplified by PCR and, again analyzed by gel electrophoresis. In many cases this method has been used to measure the levels of a particular mRNA under different conditions but the method is actually even less quantitative than PCR of DNA because of the extra reverse transcriptase step.
RT-PCR is important because it permits analysis of mRNA and therefore the study of gene transcription and easier analysis of multiple exons.

2.3.4 Real Time Polymerase Chain Reaction and TaqMan Technology

Fairly recently, a new method of PCR quantification has been invented. This is called “real-time PCR” because it allows to actually view the increase in the amount of DNA as it is amplified.
The real-time PCR system is based on the detection and quantitation of a fluorescent reporter (Lee et al., 1993; Livak et al., 1995). This signal increases in direct proportion to the amount of PCR product in a reaction. By recording the amount of fluorescence emission at each cycle, it is possible to monitor the PCR reaction during exponential phase where the first significant increase in the amount of PCR product correlates to the initial amount of target template.
The generation of PCR products can be monitored during the reaction process using fluorescently labelled probes (Lehmann and Kreipe, 2001).
There are three main fluorescence-monitoring systems for DNA amplification (Wittwer et al., 1997a): hydrolysis probes; hybridizing probes; and DNA-binding agents. DNA-binding agents, such as SYBR Green are fluorogenic dyes that exhibit little fluorescence when in solution, but emit a strong fluorescent signal upon binding to double-stranded DNA. Hydrolysis probes include TaqMan probes (Heid et al., 1996), molecular beacons (Vet & Marras, 2005) and scorpions (Terry et al., 2002). They use the fluorogenic 5' exonuclease activity of Taq polymerase

to measure the amount of target sequences in cDNA samples (Svanvik et al., 2000 for light-up probes). The TaqMan probe was used in this work to measure expression levels of genes of interest.

2.3.4.1 TaqMan probe: structure and function

The TaqMan® probe is a oligonucleotide longer than primers that contains two types of fluorophores, which are the fluorescent parts of reporter proteins (Green Fluorescent Protein (GFP) has an often-used fluorophore) (Fig. 8).

While the probe is attached or unattached to the template DNA and before the polymerase acts, the quencher (Q) fluorophore (usually a long-wavelength colored dye, such as red) reduces the fluorescence from the **reporter (R)** fluorophore (usually a short-wavelength colored dye, such as green). It does this by the use of Fluorescence (or Förster) Resonance Energy Transfer (FRET), which is the inhibition of one dye caused by another without emission of a proton. The reporter dye is found on the 5' end of the probe and the quencher at the 3' end. More used dyes are TAMRA (6-carboxytetramethylrhodamine) as reporter and FAM (6-carboxyfluorescein), or TET (tetrachloro-6-carboxyfluorescein), or JOE (2,7-dimethoxy-4,5-dichloro-6- carboxyfluorescein), or HEX (hexachloro-6-carboxyfluorescein) as quencher.

Once the TaqMan® probe has bound to its specific piece of the template DNA after denaturation (high temperature) and the reaction cools, the primers anneal to the DNA. *Taq* polymerase then adds nucleotides and removes the Taqman® probe from the template DNA. This separates the quencher from the reporter, and allows the reporter to give off its emit its energy (no more FRET). This is then quantified using a computer. The more times the denaturing and annealing takes place, the more opportunities there are for the Taqman® probe to bind and, in turn, the more emitted light is detected. This process occurs in every cycle and does not interfere with the exponential accumulation of PCR product.

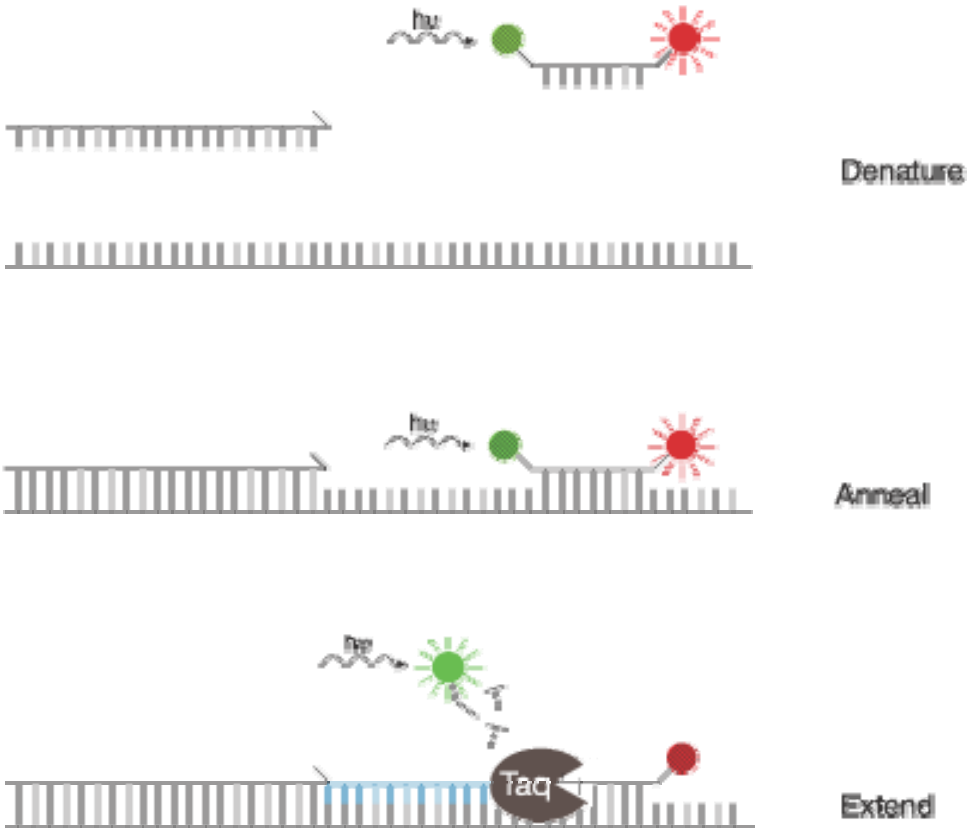

Figure 8. Three step view of the TaqMan® probe working: before the probe is met with the Taq polymerase, energy is transferred from a short-wavelength fluorophore (green) to a long-wavelength fluorophore (red). When the polymerase adds nucleotides to the template strand, it releases the short-wavelength fluorophore, making it detectable and the long-wavelength undetectable (from http://www.probes.com/handbook/boxes/0422.html)

The advantage of fluorogenic probes over DNA binding dyes is that specific hybridization between probe and target is required to generate fluorescent signal. Thus, with fluorogenic probes, non-specific amplification due to mis-priming or primer-dimer artifact does not generate signal. Another advantage of fluorogenic probes is that they can be labeled with different, distinguishable reporter dyes. By using probes labeled with different reporters, amplification of two distinct sequences can be detected in a single PCR reaction. The disadvantage of fluorogenic probes is that different probes must be synthesized to detect different sequences.

There are numerous applications for real-time polymerase chain reaction. It is commonly used for both diagnostic and research applications.

Diagnostically real-time PCR is applied to rapidly detect the presence of genes involved in infectious diseases, cancer and genetic abnormalities. In the research setting, real-time PCR is mainly used to provide highly sensitive quantitative measurements of gene transcription.

The technology may be used in determining how the genetic expression of a particular gene changes over time, such as in the response of tissue and cell cultures to an administration of a pharmacological agent, progression of cell differentiation, or in response to changes in environmental conditions.

Also, the technique is used in Environmental Microbiology, for example to quantify resistance genes in water samples.

2.3.4.2 Interpretation of gene expression results

The light emitted from the dye (reporter) in the excited state is received by a computer and shown on a graph display, such as this, showing PCR cycles on the X-axis and a logarithmic indication of intensity on the Y-axis.

Using any of the developed chemistries (hydrolysis, hybridizing probes and DNA-binding) the increase in fluorescence emission can be read by a sequence detector in “real Time”, during the course of reaction, and is direct consequence of target amplification during PCR. A computer software program calculates a ΔRn using the equation:

$$\Delta Rn = Rn^{+} - Rn^{-}$$

where Rn^{+} is the fluorescence emission of the product at each time point and Rn^{-} is the fluorescence emission of the baseline. Thus, this value expresses the probe degradation during the PCR process. The computer software constructs amplification plots using the fluorescence emission data that are collected during the PCR amplification. The ΔRn values are plotted versus the cycle number. During the early cycles of the PCR amplification, the ΔRn values do not exceed the baseline. An arbitrary threshold is chosen, based on the variability of the baseline, usually determined as 10 times the standard deviation of the baseline, set from cycles 3 to 15. Threshold cycle (C_t) values are then calculated by

determining the point at which the fluorescence exceeds this chosen threshold limit. C_t is reported as the cycle number at this point. Therefore, C_t values decrease linearly with increasing input target quantity. This can be used as a quantitative measurement of the input target (Fig. 9).

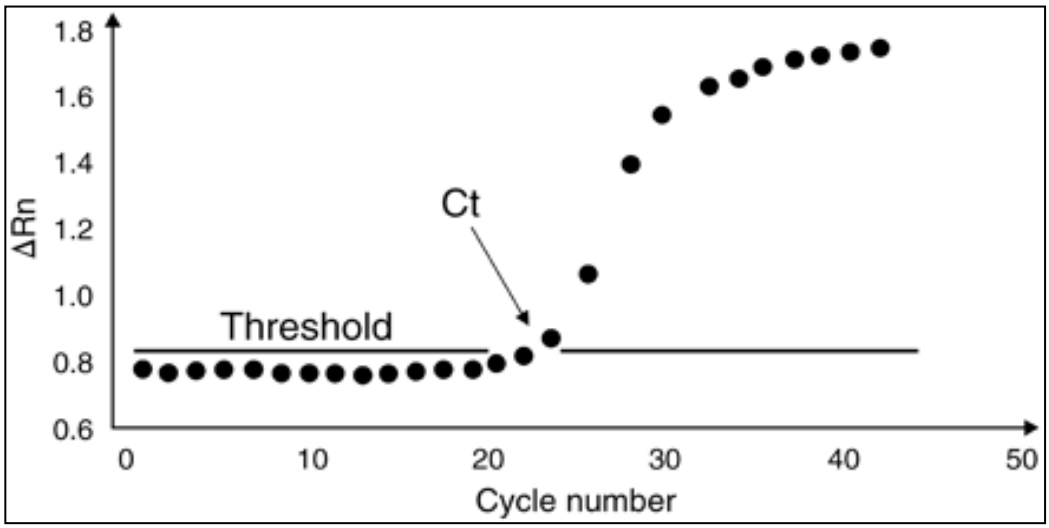

Fig.9. Example of an amplification plot.

The high specificity of this method is due to a complementary between the set of primers, the internal probe, and the target. Indeed, a fluorescence signal will be generated only if the probe is annealed to the target sequence during PCR amplification.

2.3.4.3 Quantification approaches

Generally qRT-PCR assays use one of two standard procedures: absolute or relative quantification. Absolute quantification determines the input copy number of the transcript of interest, usually by relating the PCR signal to a standard curve. Relative quantification describes the change in expression of the target gene relative to a control gene (endogenous control or housekeeping gene) or to some reference group such as an untreated control or a sample at time zero in a time-course study (calibrator). Either procedure can be applied for gene expression studies that require knowledge of how specific transcript abundance varies within a sample set.

Thus, two strategies are commonly employed to quantify the results obtained by real-time RT-PCR: the standard curve method for absolute quantitation and the comparative threshold method for relative quantitation.

Endogenous control genes

Endogenous control, or housekeeping, targets are typically constitutive RNA or DNA sequences that are present at a statistically consistent level in all experimental samples. By using the endogenous control as an active reference, the data from tha amplification of a mRNA target can be normalized for differences in the amount of total RNA adedd to each reaction. These reference genes should be consistently expressed across the samples being surveyed (e.g. developmental series, tissue set, experimental regime).

Housekeeping genes such as 18S rRNA (ribosomal RNA), β-actin, and GAPDH (glyceraldehydes-3-phosphate-dehydrogenase) are commonly used as reference genes in qRT-PCR experiments (Bustin et al., 2000 and Olsvik et al., 2005).

β-actin mRNA is expressed at moderately abundant levels in most cell types and encodes a ubiquitous cytoskeleton protein. GAPDH is ubiquitously expressed, moderately abundant message. It is frequently used as an endogenous control for quantitative RT-PCR analysis because, in some experimental systems, its expression is constant at different times and after experimental manipulation (Edwards et al., 1985). However, there is overwhelming evidence suggesting that its use as an internal standard is unappropriate (Thellin et al., 1999).

rRNAs, which constitute 85-90% of total cellular RNA, are useful internal controls, as the various rRNA transcripts are generated by a distinct polymerase (Paule et al., 2000) and their levels are less likely to vary under conditions that affect the expression of mRNAs (Barbu et al., 1989).

However, many recent studies have shown that expression levels of housekeeping genes can vary considerably within a sample set, making them unsuitable for use as reference genes for data normalization in qRT-PCR (Dhar et al., 2002; Tricarico et al., 2002; Vandesompele et al., 2002; Perez-Novo et al., 2005; and de la Vega, 2006).

Selection of suitable reference genes is not a simple process. It is desirable to validate the chosen normalizer for the target cell or tissue. It should be expressed at a constant level at different time points by the same individual and also by different individuals at the target cell or tissue (Dheda, 2004). For this reason, reference genes for can be reliably selected from microarray expression data (Woods et al., 2004) or from high-throughput qRT-PCR assays (ABI TaqMan Rat Endogenous Control Panel) which allow rapid screening of a large number of housekeeping genes evaluate the expression of select genes.

3 MATERIALS AND METHODS

3.1 Test Articles

Hexachloro-1:3-butadiene (HCBD, purity >97%), potassium dichromate ($K_2Cr_2O_7$), and Cephaloridine hydrate were supplied by Sigma Chemical Co. (St. Louis, Mo., USA).

3.2 Animals and treatment

Investigations were performed on different aged Albino male Wistar rats (C. River), kept under standardized conditions, fed with standard diet (Nuova Zoofarm, Italy) and drink ad libitum.

HCBD was dissolved in corn oil, $K_2Cr_2O_7$ and Cephaloridine were dissolve in sterile saline. Doses were selected on the basis of literature information (Trevisan et al., 1999; Kurota and Yamaguchi, 1995). Details on animals and treatments are reported in Tables 2, 3 and 4.

		Group number	Animals/group	Treatment Vehicle/Test Compound	Test Compound Dose (mg/kg body wt)	Somministration	Animal age
Ageing Study	1 experiment	1	4	Corn Oil	0	i.p.	6 weeks
		2	4	Sterile Saline	0	s.c.	6 weeks
		3	4	HCBD (in Corn oil)	100	i.p.	6 weeks
		4	4	$K_2Cr_2O_7$ (in Sterile Saline)	25	s.c.	6 weeks
	2 experiment	5	4	Corn Oil	0	i.p.	14 weeks
		6	4	Sterile Saline	0	s.c.	14 weeks
		7	4	HCBD (in Corn oil)	100	i.p.	14 weeks
		8	4	$K_2Cr_2O_7$ (in Sterile Saline)	25	s.c.	14 weeks
	3 experiment	9	4	Corn Oil	0	i.p.	26 weeks
		10	4	Sterile Saline	0	s.c.	26 weeks
		11	4	HCBD (in Corn oil)	100	i.p.	26 weeks
		12	4	$K_2Cr_2O_7$ (in Sterile Saline)	25	s.c.	26 weeks
	4 experiment	13	4	Corn Oil	0	i.p.	38 weeks
		14	4	Sterile Saline	0	s.c.	38 weeks
		15	4	HCBD (in Corn oil)	100	i.p.	38 weeks
		16	4	$K_2Cr_2O_7$ (in Sterile Saline)	25	s.c.	38 weeks
	5 experiment	17	4	Corn Oil	0	i.p.	48 weeks
		18	4	Sterile Saline	0	s.c.	48 weeks
		19	4	HCBD (in Corn oil)	100	i.p.	48 weeks
		20	4	$K_2Cr_2O_7$ (in Sterile Saline)	25	s.c.	48 weeks

Table 2: Group number, animals/group, treatment, doses, somministration route and animal age for ageing study with HCBD and $K_2Cr_2O_7$ (Phase I).

		Group number	Animals/group	Treatment Vehicle/Test Compound	Test Compound Dose (mg/kg body wt)	Somministration	Animal age
Dose-Response Study	6 experiment	21	4	Corn Oil	0	i.p.	8 weeks
		22	4	HCBD (in Corn oil)	100	i.p.	8 weeks
		23	4	HCBD (in Corn oil)	50	i.p.	8 weeks
		24	4	HCBD (in Corn oil)	25	i.p.	8 weeks
	7 experiment	25	4	Sterile Saline	0	s.c.	8 weeks
		26	4	$K_2Cr_2O_7$ (in Sterile Saline)	25	s.c.	8 weeks
		27	4	$K_2Cr_2O_7$ (in Sterile Saline)	12.5	s.c.	8 weeks
		28	4	$K_2Cr_2O_7$ (in Sterile Saline)	8	s.c.	8 weeks

Table 3: Group number, animals/group, treatment, doses, somministration route and animal age for dose range studies with HCBD and $K_2Cr_2O_7$ (Phase I).

		Group	Animals/group	Treatment	Test Compound Dose	Somministration	Animal age
		number		Vehicle/Test Compound	(mg/kg body wt)		
Dose-response study	8 experiment	29	4	Sterile Saline	0	i.p.	8 weeks
		30	4	Cephaloridine (in Sterile Saline)	100	i.p.	8 weeks
		31	4	Cephaloridine (in Sterile Saline)	50	i.p.	8 weeks
		32	4	Cephaloridine (in Sterile Saline)	25	i.p.	8 weeks

Table 4: Group number, animals/group, treatment, doses, somministration route and animal age for dose range study with Cephaloridine (Phase II).

3.3 Tissue collection

At necropsy, each rat was euthanized with isofluorane and a sample of blood was collected from heart in eparinized tubes, centrifuged for 10 min at approximately 2000 g and plasma was used for standard clinical chemistry analysis.

Upon the removal of the kidneys, the wright kidney was cut transversally into three portion, a central and two peripheral. The central was placed in 10% neutral buffered formalin for histopathology. From one peripheral portion, $3mm^3$ pieces (cortical region) was sampled, fixed and stored in 4% formaldehyde/1% gluteraldehyde in phosphate buffer solution for possible future Electron Microscopy investigations. The last peripheral portion was frozen into cold N-Hexane and stored at -80°C for possible future immunohistochemical analysis. The left kidney was collected and chopped into smaller pieces (~3-5 mm^3) (cortical region), collected into 5 mL RNALater reagent and stored at -80C for gene expression measurement.

All animals received complete post-mortem examination for gross abnormalities during collection of tissues for histopathologic evaluation and RNA exctraction.

3.4 Clinical Chemistry

The traditional clinical chemistry parameters of nephrotoxicity, BUN and creatinine, were measured using an automated chinical chemistry analyzer (ADVIA 1650 Chemistry System, Siemens).

The method for BUN quantification is based on Talke and Schubert enzymatic procedure (1965) for determination of urea using the coupled urease/glutamate dehydrogenase (GLDH) enzyme system. The assay has been optimized for analyzers that permit kinetic (fixed-time) measurements.

After addion of a buffer/NADH and buffer/enzymes/substrate reagents to the sample, urea is hydrolyzed by urease to form CO2 and ammonia. The ammonia formed then reacts with α-ketoglutarate and NADH in the presence of GLDH to yield glutamate and NAD^+. The decrease in absorbance due to consumption of NADH is measured kinetically (2 points-kinetic enzymatic UV method).

Creatinine determination method in the plasma is based on Jaffe' reaction as described by Popper and Mandel (1937). In alkaline solution, creatinine forms a yellow-orange complex with picrate. The color intensity is directly proportional to the creatinine concentration and can be measured photometrically (1 point-kinetic colourimetric method).

3.5 Histology

Kidney section for histology was fixed in 10% neutral buffered formalin.

Within 48 hours of placement in formalin, kidney samples were dehydrated by passage through serial baths of graded alcohol and toluene. The dehydrated samples were embedded in paraffin, and 3 μm-thick sections were stained by hematoxylin and eosin (H&E) and Periodic Acid Schiffs (PAS).

At microscopic examination, tubular cell degeneration, necrosis, regeneration were graded as minimal to marked according to the percentage of tubules involved (Minimal: 10-20%; Mild: 30-50 %; Moderate: 60-70 %, Marked: 80-100%).

The severity of tubular dilation with scattered cell degeneration/cast/debris was graded according to the extension of the damage (Minimal: cortex only; Mild:

cortex to outer medulla; Moderate: cortex to upper portion of inner medulla; Marked: cortex to deep portion of inner medulla (papilla)).

3.6 Gene Expression

Details for consumables for gene expression processing is reported in Table 5.

Category	Consumable	Source
RNA Isolation, quantity/ quality checks	RNALater™	Ambion (Europe) Ltd via CELBIO S.p.a., Milano, Italy
	TRIzol Reagent	Invitrogen S.R.L., Milano, Italy
	RNeasy Mini kit	Qiagen S.p.A., Milano, Italy
	6000 Nano Reagents & Supplies Kit	Agilent Technologies S.p.a., Milano, Italy
	RiboGreen™ Assay Kit	Invitrogen S.R.L., Milano, Italy
DNase Treatment and cDNA Synthesis	DNase 1 RNase-free	Ambion (Europe) Ltd via CELBIO S.p.a., Milano, Italy
	Superase-Inhibitor	Ambion (Europe) Ltd via CELBIO S.p.a., Milano, Italy
	Nuclease-free water	Invitrogen S.R.L., Milano, Italy
	96-well Optical Reaction Plate	Applera Italia, Monza, Mi, Italy
	High Capacity cDNA Archive Kit	Applera Italia, Monza, Mi, Italy
	RT Random Primers	Applera Italia, Monza, Mi, Italy
	dNTP Mix (10 mM)	Applera Italia, Monza, Mi, Italy
TaqMan™ qRT-PCR	Low Density Array Rat Endogenous Control Panel	Applera Italia, Monza, Mi, Italy
	KIM-1, Cln, Rgn, Spp1 Gene Expression Assays	Applera Italia, Monza, Mi, Italy
	Universal PCR Mix	Applera Italia, Monza, Mi, Italy
	96-well Optical Reaction Plate	Applera Italia, Monza, Mi, Italy
	Optical PCR Film	Applera Italia, Monza, Mi, Italy

Table 5. List of consumables used for gene expression processing.

3.6.1 RNA isolation

Rat kidney samples stored in RNALater at -80°C were weighed and eventually cut to obtain a piece of approximately 30 mg. RNA isolation and purification was performed using the RNeasy Mini kit (Qiagen).

Each sample was homogenised in 600 µL Buffer RLT using the Qiagen Tissue Lyser. An equal volume of 70% (v/v) ethanol was added to the homogenized lysate. The mixture was transferred to mini RNeasy column and centrifuged for 15 s at 11,000 g. After discarding the flowthrough, 700 µL Buffer RW1 were added to the RNeasy colum and centrifuged for 15 s at 11,000 g to wash the column. The RNeasy column was then transferred into a new collection tube and 500 µL Buffer RPE were added to the column and centrifuged for 15 s at 11,000 g to wash the column. This step was repeated twice. To elute RNA, 50 µL RNase-free water were added to the column and centrifuged for 1 min at 11,000 g.

3.6.2 RNA quantity check

Total RNA was roughly quantified by UV spectrophotometer (Eppendorf) measuring the absorbance at 260 nm (A_{260}). Both RNA and DNA absorb UV light making it possible to detect and quantify either at concentrations as low as 2.5 ng/µl. The nitrogenous bases in nucleotides have an absorption maximum at about 260 nm. Using a 1-cm light path, the extinction coefficient for nucleotides at this wavelength is 20. Based on this extinction coefficient, the absorbance at 260 nm in a 1-cm quartz cuvette of a 50µg/ml solution of double stranded DNA or a 40µg/ml solution of single stranded RNA is equal to 1. For this reason, the RNA concentration in a sample can be calculated as follows:

RNA concentration (µg/ml) = (A_{260}) x (dilution factor) x (40 µg RNA/ml)/(1 A_{260} unit)

Absorbace was also measured at 280nm so that A 260/280 for each sample could be calculated to give an indication of sample purity. In contrast to nucleic acids, proteins have a UV absorption maximum of 280 nm, due mostly to the tryptophan residues. The absorbance of a DNA sample at 280 nm gives an estimate of the protein contamination of the sample. The ratio of the absorbance at 260 nm/ absorbance at 280 nm could be calculated to give an indication of sample purity. It should be between 1.65 and 1.85.

3.6.3 DNAsing treatement

To eliminate any possible genomic DNA contamination, samples were treated with DNase 1 enzyme (Ambion). To 20μg RNA were added 4U DNase, 20 U Superase and nuclease-free water to a final volume of 50 μl. Samples were incubated in a thermocycler for 10 minutes at 37°C, followed by 5 minutes at 75°C.

3.6.4 DNased RNA quality check

DNased RNA quality was checked by the Bioanalyzer 2100 (Agilent Technologies), using a RNA 6000 Nano kit. The Bioanalyzer allows the evaluation of RNA status (degradation) by a micro-electrophoretic analisys on a chip. Since the majority of RNA (approximately 80%) in the samples is ribosomal and RNase activity digests RNA to give smaller fragments, this can be detected by electrophoresis.

A gel-dye mix was prepared by adding 1 μL of dye concentrate into 65 μL of filtered gel and then centrifuged at 13,000g for 10 minutes. The gel-dye mix was loaded into a chip and 5 μL of a heat denatured ladder and 1 μL of heat denatured samples (approximately 200 ng) were pipetted into specific wells together with 5 μL marker. For optimal performance of the total RNA (6000 Nano) assay, sample RNA concentration should be 5-500 ng/μL. The chip was vortexed for 1 min at 2400 rpm and run on the Agilent 2100 Bioanalyser instrument.

The Bioanalyzer provides a platform that uses a fluorescent assay involving electrophoretic separation to evaluate RNA samples qualitatively. The Bioanalyzer measures the amount of fluorescence as the RNA sample is pulsed through a microchannel over time. The software creates a graph called an electropherogram, which diagrams fluorescence over time. For each sample the software creates a gel image to accompany the graph. Smaller molecules are pulsed through the separation channel quicker than larger ones and will therefore appear on the left side of the electropherogram.

The gel view of the electrophoresis should show two clear bands due to the 18S and 28S ribosomal RNAs (Fig.10).

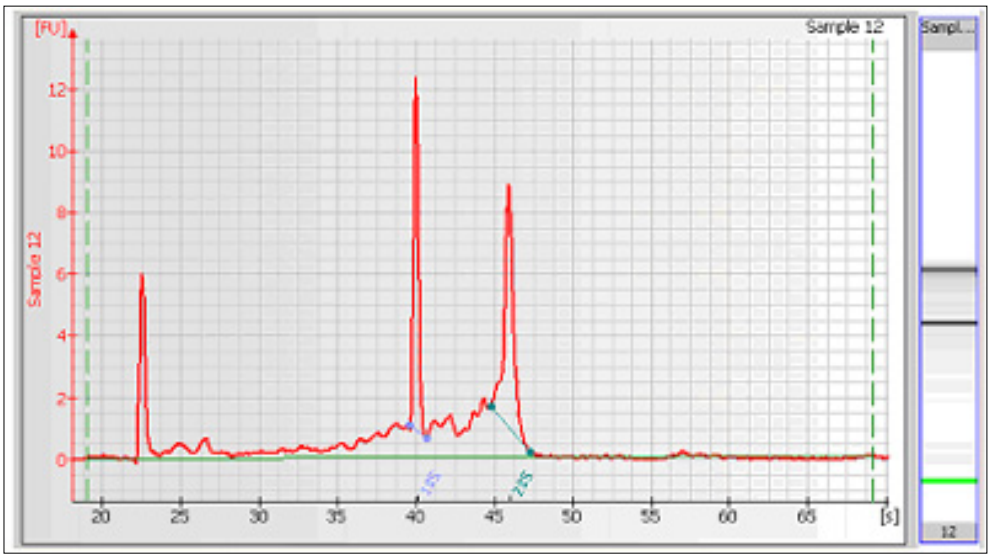

Fig.10. Example of high quality RNA sample electropherogram and gel image (showing 3 peaks corresponding to marker, 18S and 28S ribosomal units, respectively).

3.6.5 DNased RNA quantity check by RiboGreen™ assay

DNased RNA was quantified using the RiboGreen™ RNA Quantitation Kit (Molecular Probes, Leiden) to have an exact value of RNA in each sample for cDNA synthesis.This is a fluorescent probe that binds nucleic acids specificly and gives a direct quantification of RNA by fluorescence detection.

Aliquots of 1x TE buffer were distributed into appropriate wells on a 96-well plate. Ribosomal RNA was used to make a standard curve with final concentrations ranging from 0 to 200 ng/mL. Aliquots of diluted (from 1:2000 to 1:64000) total RNA isolates were added into subsequent wells followed by the addition of the fluorescent RNA binding reagent (100 µL, using a 1 in 2000 dilution of stock in 1x TE buffer) into wells whether containing samples or standards. The 96-well optical reaction plate was sealed with optical PCR film followed by centrifugation for 1 minute. The fluorescence in each well was measured using the a plate fluorescence reader (SpectraMax Gemini XPS, Molecular Devices) with λ-480 nm excitation and λ-520 nm emission. The concentrations of the total RNA isolates were interpolated from the standard curve.

3.6.6 Reverse-Transcriptase PCR (cDNA sinthesys)

Synthesis of the cDNA template was based on the ABI High Capacity cDNA Archive Kit. Reverse transcription was carried out in the presence (RT+) and absence (RT-) of the Superscript II reverse transcriptase enzyme. The RT- sample was prepared to allow the identification of eventual genomic DNA contamination. RT+ samples were created in duplicate (a and b) to evaluate variability caused by RT-PCR reaction. Nuclease-free water was added for the no template control samples (NTC) into the 96-well plate of the DNase treated samples.

On the basis of RiboGreen™ measurements, 4 μg RNA were added to an appropriate volume of nuclease-free water to make the total volume equal to 70 μL. Aliquots of the master mix [30 μL per well, 10X RT Buffer (10 μL), 10X RT Random Primers (10mμL), 100mM dNTP (4 μL), 50U/μL Multi-Scribe RT (5 μL) and 20U/μL Superase-Inhibitor (1 μL)] were added to 70 μL RNA.

The plate was sealed with adhesive PCR film, centrifuged for 1 minute at 4°C, incubated at room temperature for 10 min and heated to 37°C for 2 hours.

Samples were stored at -20ºC until required.

3.6.7 Endogenous control (housekeeping) gene selection by Low Density Array

For meaningful gene expression measurement, an endogenous control or housekeeping gene, with constant expression level is essential to control for differences between samples. For this purpose the TaqMan Low Density Array Rat Endogenous Control Panel (Applied Biosystems, ABI) was used because it allows a rapid screening of many samples across many genes. It consists of the most commonly used housekeeping genes that are provided as a pre-formulated set of pre-designed probe and amplification primers (TaqMan gene expression assay). Different 16 rat housekeeping genes were screened (Table 6).

Each TaqMan gene expression assay consists of a fluorogenic FAM™ dye-labeled MGB (minor groove binder) probe and two amplification primers (forward and reverse) provided in a pre-formulated 20X mix; 1X final

concentrations are 250 nM for the probe and 900nM for each primer. Each assay has an amplification efficiency of 100% +/- 10%. Each assay on the Low Density Array is spotted in triplicate into the 384 wells.

For HKGs screening, 12 samples from the first experiment of the ageing study using HCBD and $K_2Cr_2O_7$ (validation phase) were used (Table 2). Each cDNA (40 ng/μL) prepared from total RNA was diluted with RNase/DNase-free water and 2X TaqMan™ Universal PCR Master Mix to a final concentration of 1 ng cDNA/μL. Next, 100 μL of each single sample was loaded into one of the eight sample ports of the TaqMan Low Density Array Endogenous Control Panel. Two Low Density Arrays were used for this purpose, for running HCBD and $K_2Cr_2O_7$ samples, respectively. Each array loaded with the sample-specific PCR mix was sealed and cut off the fill reservoirs, centrifuged twice at 1000 rpm for 1 min to distribute the PCR mix into the wells, and placed into the ABI 7900 HT (Applied Biosystems) with 384-plate block (Fig.11). The instrument heated to 50°C for 2 minutes, ramped to 95°C for 10 minutes followed by 40 cycles of 95°C for 0.15 minutes and 60°C for 1 minute.

Figure 11. A real-time PCR machine (ABI7900HT)

3.6.8 TaqMan™ Real Time-PCR

Specific TaqMan™ Gene Expression Assays were used to quantify KIM-1, Cln, Rgn and Spp1. These assays consist of a 20X mix of unlabeled PCR primers and TaqMan™ MGB probe (FAM™ dye-labeled). They are designed for the detection and quantitation of specific genetic sequences in RNA samples converted to cDNA.

Besides target genes (KIM-1, Cln, Rgn and Spp1), also an endogenous control gene (18S ribosomal RNA) resulted from the TaqMan Low Density Array Rat Endogenous Control Panel screening, was evaluated as an active reference.

For each gene of interest a mastermix was prepared. The mastermix contained 1 µL gene specific 20X TaqMan™ Gene Expression Assays, 10 µL 2X TaqMan™ Universal PCR Master Mix and 4 µL RNase/DNase-free water. 15 µL of mastermix was then added into each well of a 96 well optical reaction plate which contained 5 µL of the relevant template: RT+ a, RT+ b, and RT- cDNA. Reactions used cDNA from the equivalent of 40 ng RNA. Each plate contained also 12 no template control (NTC) wells to monitor non-specific priming and mastermix contamination. To generate a standard deviation for the relative quantity value of a target, each plate contained three replicates of the target and endogenous control. The 96-well optical reaction plate was sealed with optical PCR film followed by centrifugation for 1 minute. The plate was then placed into the ABI 7900HT instrument and heated to 50°C for 2 minutes, ramped to 95°C for 10 minutes followed by 40 cycles of 95°C for 0.15 minutes and 60°C for 1 minute.

3.6.9 Gene expression data evaluation

The amplification plots were evaluated using the RQ Manager Software (ABI). This tool used for gene expression quantification supports real-time relative quantification of nucleic acids using the comparative C_t method.

This method uses the following arithmetic formula to achieve results for relative quantification, expressed as relative amount of mRNA (RQ):

$$2^{-\Delta\Delta Ct}$$

where:

$\Delta\Delta C_t$ = the normalized signal level in a sample relative to the normalized signal level in the corresponding calibrator sample. The normalized signal levels refer to the signals generated by the amplification of the target sequence in the unknown and calibrator samples which is normalized to the signal generated by the amplification of the endogenous control.

The purpose of the internal control gene is to normalize the PCR products for the amount of RNA added to the reverse-transcription reactions.

As calibrator an untrated control was chosen for each experiment and it was analyzed on every assay plate with the other samples for both target and endogenous control genes.

The $\Delta\Delta C_t$ method is validated by demonstrating that the efficiency of the target amplification (gene of interest) and the efficiency of the endogenous control amplification (HKG) are comparable or equal.

3.6.10 Statistical analysis

Data were analyzed for statistical difference ($p < 0.05$, $p < 0.01$) between control and treated groups, using Statistica version 6.0 software. ANOVAs followed by Dunnett's *t* test were performed on sample means.

All data from plasma clinical chemistry and kidney gene expression were expressed as means +/- standard deviation (SD) and analyzed using Dunnett's *t* test.

Reference intervals for each gene were calculated in control animals treated with corn oil (HCBD vehicle) or sterile saline ($K_2Cr_2O_7$ or Cephaloridine vehicle) using the Statistica version 6.0 software.

Gene Symbol	Gene Name	Context Sequence	Category
Actb	actin, beta	CCTTCCTTCCTGGGTATGGAATCCT	Cytoskeletal protein
Arbp	acidic ribosomal phosphoprotein P0	TTCCTTAAGATCATCCAACTTTTGG	Nucleic acid binding
B2m	beta-2 microglobulin	GTGCTTGCCATTCAGAAAACTCCCC	Defense/immunity protei
18S	Eukaryotic 18S rRNA	TGGAGGGCAAGTCTGGTGCCAGCAG	Molecular function unclass
Gapdh	glyceraldehyde-3-phosphate dehydrogenase	AACCCATCACCATCTTCCAGGAGCG	Oxidoreductase
Gusb	glucuronidase, beta	TTACTTCAAGACGCTGATCGCCCAC	Hydrolase
Ppia	peptidylprolyl isomerase A	GGATTCATGTGCCAGGGTGGTGACT	Isomerase
Ppib	peptidylprolyl isomerase B	CTACAGGAGAGAAAGGATTTGGCTA	Isomerase
Hprt	hypoxanthine guanine phosphoribosyl transferase	CAGGGATTTGAATCATGTTTGTGTC	Transferase
Tbp	TATA box binding protein	CCCACCAGCAGTTCAGTAGCTATGA	Transcription factor
Hmbs	hydroxymethylbilane synthase	TCTGCAAACGGGAAAACCCTTGTGA	Hydrolase
Ywhaz	tyrosine 3-monooxygenase/tryptophan 5-monooxygenase activation protein, zeta polypeptide	CTGCAACGACGTACTGTCTCTTTTG	Miscellaneous function
Pgk1	phosphoglycerate kinase 1	ACCTGCTGGCTGGATGGGCTTGGAC	Kinase
Rplp2	ribosomal protein, large P2	TGTCATCGCTCAGGGTGTTGGCAAG	Nucleic acid binding
Tfrc	transferrin receptor	GTTTTTGTGAGGATGAGGACTATCC	Molecular function unclass
Ubc	ubiquitin C	TCTTGGGTTTGATGGGGAGGTGTCT	Molecular function unclass

Table 6: TaqMan Low Density Array Rat Endogenous Control Panel details.

4 RESULTS

4.1 Phase I

4.1.1 Ageing study

4.1.1.1 Gene expression

Kidney sample of male rats treated with a single injection of 100 mg/kg HCBD and 25 mg/kg $K_2Cr_2O_7$ at different ages (6-, 14-, 26-, 38- and 48-week-old) were collected at 48h after dosing and processed through gene expression quantification following the different steps listed in scheme 1, such as tissue homogenization, RNA isolation, quantity check (absorbance), DNase treatment, quality and quantity check and cDNA synthesis.

An endogenous control (housekeeping) gene was selected using samples from the first experiment of ageing study. Ideally, the internal control gene for quantitative gene expression studies should not be influenced by the conditions of the experiment. To identify the best candidate gene to use as endogenous control for normalization, the expression profile of different 16 rat housekeeping genes (Table 6) was determined for fourteen animals, 6-week-old, treated with 100 mg/kg HCBD and 25 mg/kg $K_2Cr_2O_7$ and related controls (Table 2). Each Taqman assay was run in triplicate for each sample. The average C_t with standard deviation (SD) for each sample was calculated and showed in Fig 12 for HCBD and in Fig. 12 for $K_2Cr_2O_7$.

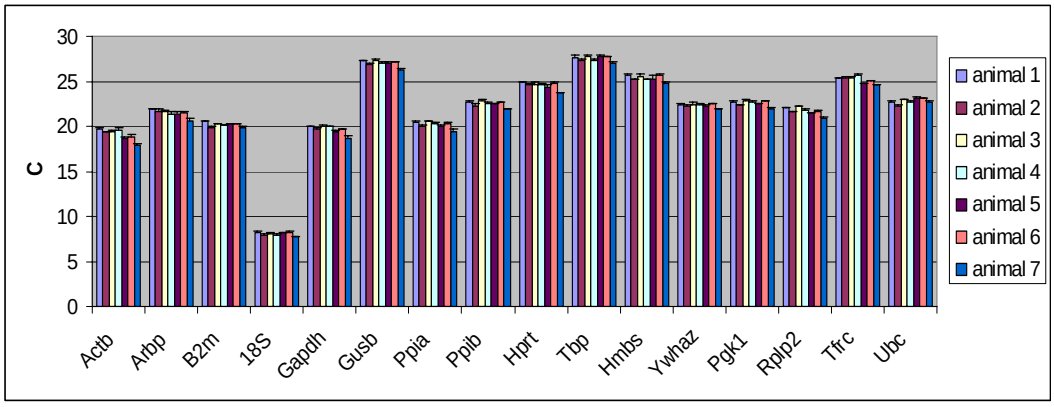

Fig.12. mRNA expression of 16 putative rat endogenous controls across 7 samples (1-3 controls; 4-7 HCBD treated animals). Each bar represents one individual and measures the average C_t (n=3); error bars are SD.

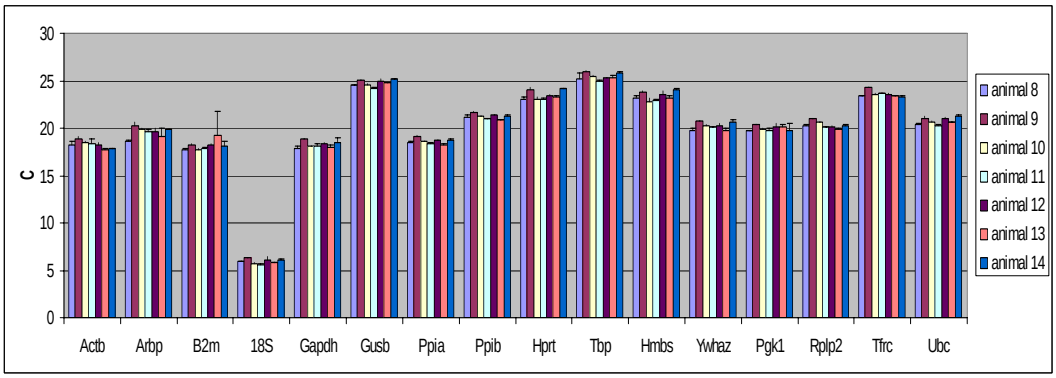

Fig.13. mRNA expression of 16 putative rat endogenous controls across 7 samples (8-10 controls; 11-14 $K_2Cr_2O_7$ treated animals). Each bar represents one individual and measures the average C_t (n=3); error bars are SD.

The average C_t was then used to determine the average C_t and SD of C_t for each gene across the different samples. This SD was used to identify the gene with the least variation amongst the 16 genes examined (Fig.14 and 15).

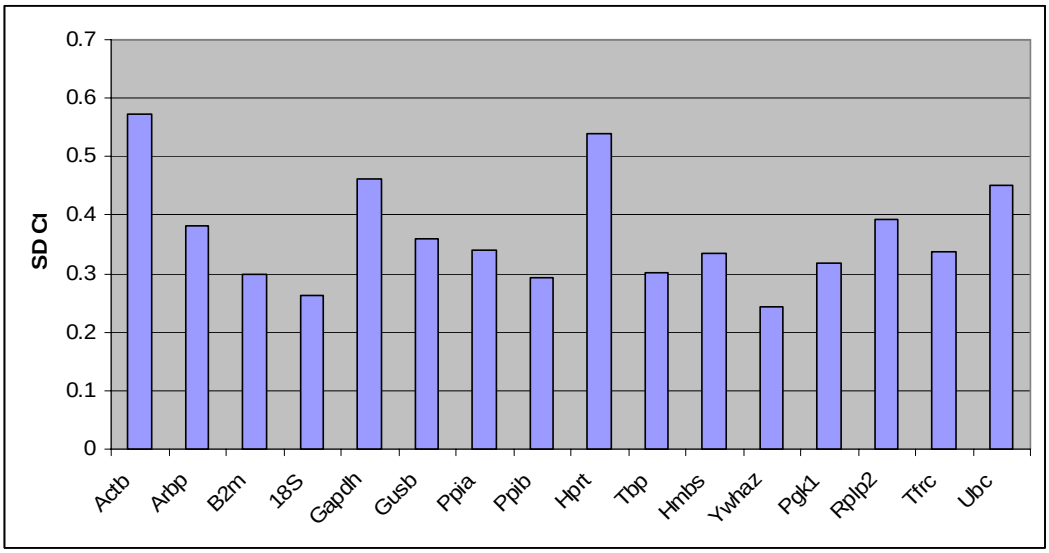

Fig.14. Variation of 16 rat endogenous controls across 7 samples (1-3 controls; 4-7 HCBD treated animals) as measured by SD of Ct.

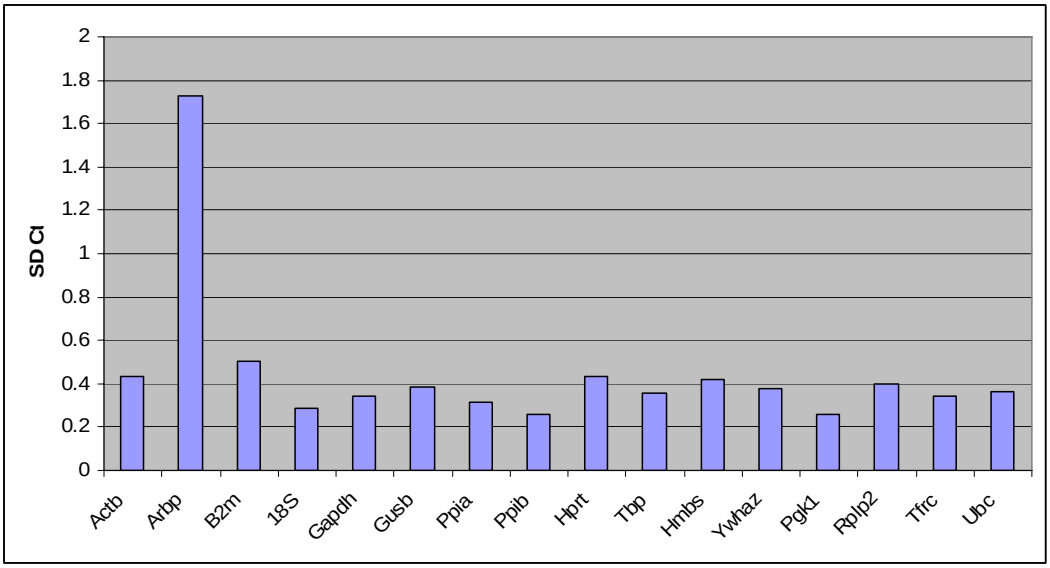

Fig.15. Variation of 16 rat endogenous controls across 7 samples (8-10 controls; 11-14 $K_2Cr_2O_7$ treated animals) as measured by SD of Ct.

From these data, the rat endogenous control genes with the lowest SD in 6-week-old control and HCBD and $K_2Cr_2O_7$ treated animals, and therefore, the lowest variation across samples, was 18S (0.26 for HCBD and 0.28 for $K_2Cr_2O_7$ experiment). Thus, 18S appears to be the best candidate to serve as endogenous control under both conditions.

After endogenous control gene selection, the 4 genes of interest were evaluated in animals at different ages (6-, 14-, 26-, 38- and 48-week-old) treated with HCBD 100 mg/kg and $K_2Cr_2O_7$ 25 mg/kg and their expression was normalized to 18S gene transcript to obtain relative amount of mRNA (RQ) for each gene.

Variability in the expression of KIM-1, Cln, Rgn and Spp1 within control animals, at different ages, treated with corn oil (HCBD vehicle) or sterile saline ($K_2Cr_2O_7$ or Cephaloridine vehicle) was evaluated by the variance analysis (ANOVA) test. Results showed no significant differences in gene expression for each gene in the 2 vehicle groups (Fig. 16, 17, 18, 19, 20). Moreover, no significant difference was evidenced with ageing.

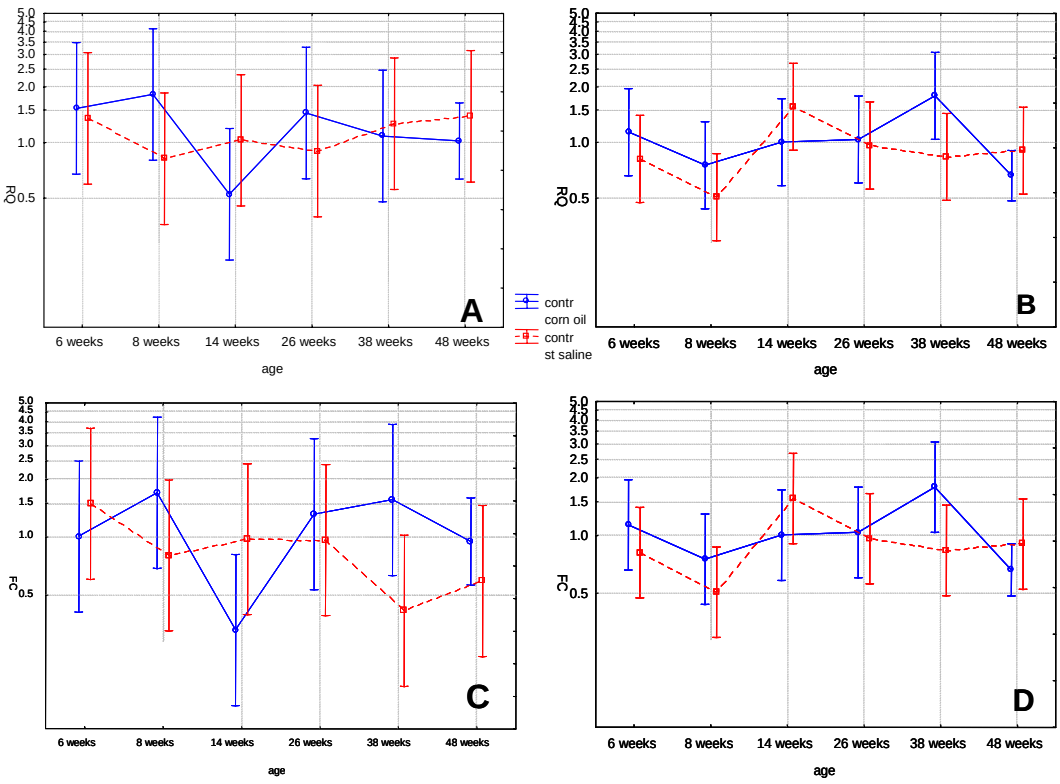

Fig.16. KIM-1 (A), Cln (B), Spp1 (C) and Rgn (D) expression (LogRQ) in control rats (corn oil and sterile saline groups) at different ages.

To evaluate the biological significance in gene expression changes, reference intervals for each gene were calculated for all control animals treated both with corn oil and sterile saline, using the normal distribution and the non-parametrical percentile methods. Reference intervals were calculated so that contain 95% of the test population (controls gene expression values).
On the basis of this analysis, the following thresholds were obtained: 2.8 for KIM-1, 1.5 for Cln, 2.5 for Spp1, and 0.4 for Rgn. Gene expression responses were considered biologically significant for changes in the appropriate direction (up-regulation for KIM-1, Cln and Spp1; down-regulation for Rgn) and magnitude from control in at least three out of four animals in the treated groups.

The age-dependent effects of HCBD and $K_2Cr_2O_7$ on the four putative gene expression markers of nephrotoxicity were assessed. The transcript levels of the four genes in kidney tissue were compared to age-matched controls. Statistical significance was determined based on analysis of the group means using an ANOVA with a Dunnett's *t* test.

Expression results for all genes, as fold changes, obtained in the HCBD ageing study are reported in Fig. 17.

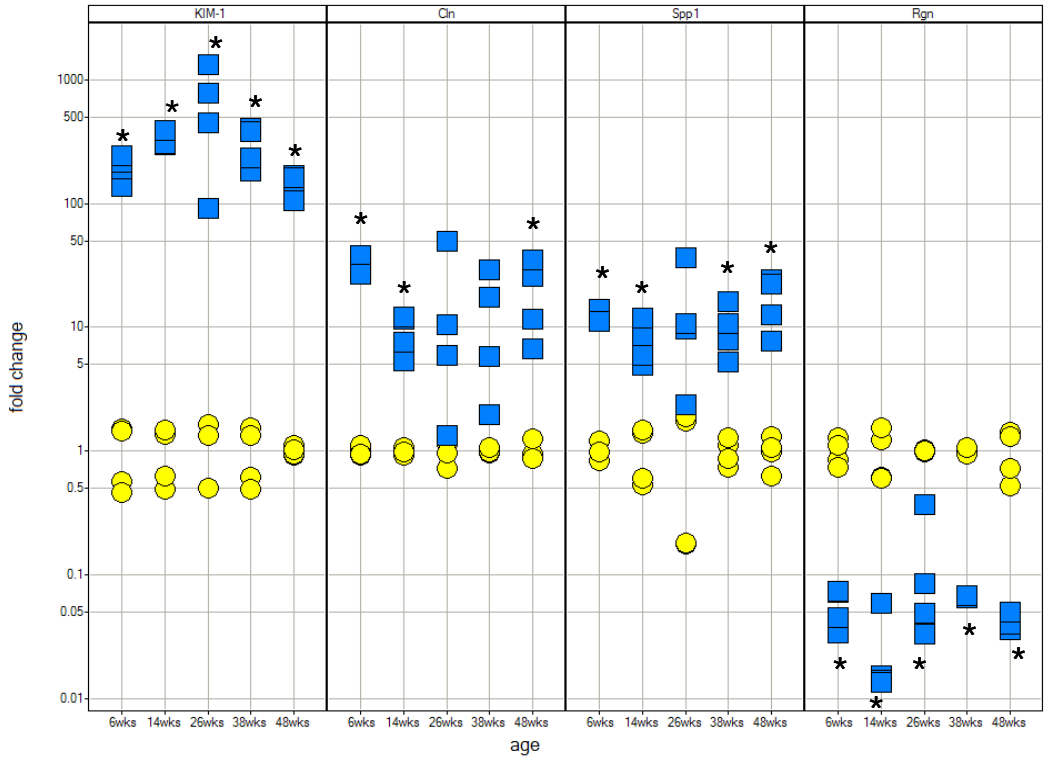

Fig.17. KIM-1, Cln, Spp1, and Rgn mRNA expression (fold change). Transcript levels are shown for individual animals treated with a single i.p. injection of 100 mg/kg HCBD (blue box, n = 4) within each age group of 6-, 14-, 26-, 38-, or 48-week-old rats relative to average level in controls (vehicle: corn oil, yellow circle, n = 4). Statistical significance in a Student's *t* test comparison of age-matched treated and control values is indicated (*p < 0.05).

KIM-1 mRNA levels were significantly increased in all treated groups, up to 660-fold over control at 26 weeks of age.

Clusterin expression increased in all treatment groups, although statistical significance was noted only in 6-, 14- and 48-week-old rats. The range for HCBD-induced Cln gene expression changes was more than an order of magnitude lower compared to HCBD-induced KIM-1 expression changes.

Spp1 was observed to have expression patterns similar to clusterin since it showed an increased expression in all groups of treatment, not statistically significant in the 26-week-old group only, due to the variability within this group.

Treatment with HCBD induced down-regulation of Rgn transcript, statistically significant in all groups.

The observed effect of treatment on the level and significance of change in genes associated with nephrotoxicity suggested a difference in sensitivity with the age for KIM-1 only, that showed the following order: 26-week-old » 14-and 38-week-old > 6-week-old > 48-week-old.

For the other genes, any difference in sensitivity to HCBD-induced renal damage in the five age groups was assessed. For two genes, Cln and Spp1, the increase was not statistically significant at 26 weeks due to variability in the expression of these genes within this group (caused by animal no.31) that accounted for the lack of statistical differences compared to controls, although the mean fold changes at 26 weeks were 17- and 15-fold over control, respectively.

Expression results for all genes, as fold changes, obtained in the $K_2Cr_2O_7$ (25 mg/kg) ageing study are reported in Fig. 18.

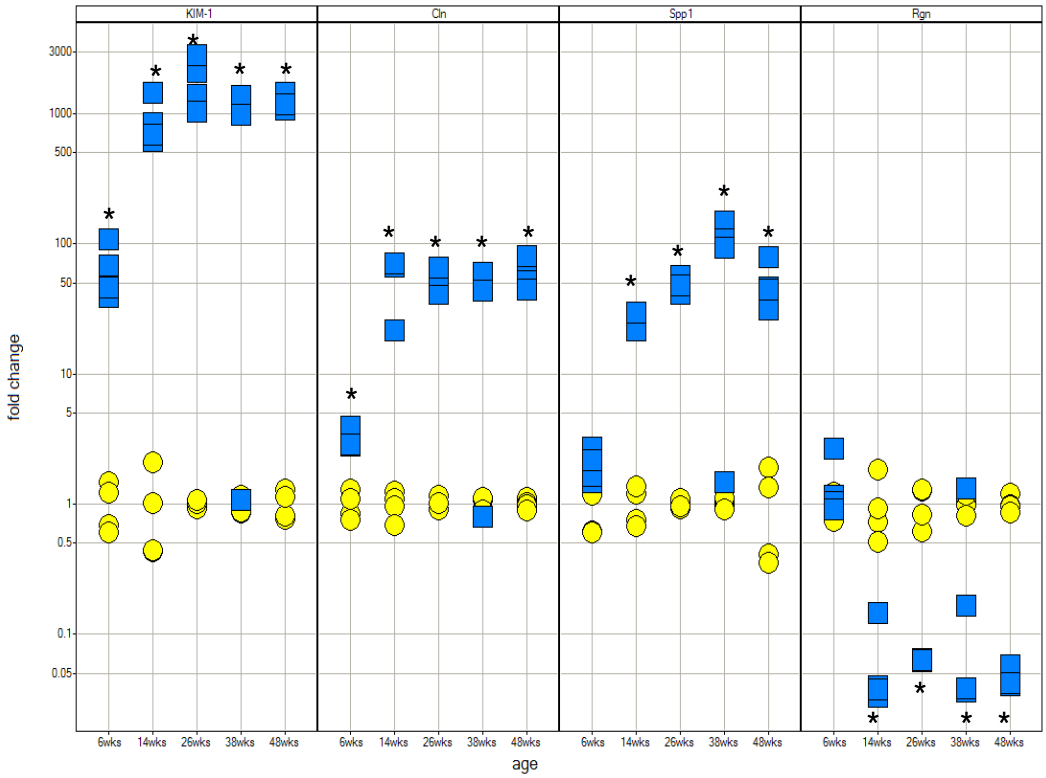

Fig.18. KIM-1, Cln, Spp1, and Rgn mRNA expression (fold change). Transcript levels are shown for individual animals treated with a single s.c. injection of 25 mg/kg $K_2Cr_2O_7$ (blue box, n = 4) within each age group of 6-, 14-, 26-, 38-, or 48-week-old rats relative to average level in controls

(vehicle: corn oil, yellow circle, n = 4). Statistical significance in a Student's *t* test comparison of age-matched treated and control values is indicated (*p < 0.05).

Treatment caused statistically significant increased expression of KIM-1 in all the age groups. One animal in the 38-week-old group (an.53) showed a gene expression value similar to controls. The range of drug-induced changes in KIM-1 gene expression was greater than HCBD, starting from 14-week-old group up to 1800-fold at 26 weeks, even if at 6 weeks of age, treated animals showed an increase of 65-fold, lower than HCBD at the same age-point.

Cln expression was significally increased in all groups of treatment, up to 63-fold increase at 48 weeks of age. Also in this case, the $K_2Cr_2O_7$-induced increased gene expression was greater than HCBD starting from 14 weeks of age. No difference with controls values were observed for one rat in the 38-week-old group.

Spp1 mRNA levels were significantly increased starting from 14-week-old group, up to 88-fold over control at 38 weeks of age, even though for one animal in this group no difference with controls values were observed (an. 53).

Treatment with $K_2Cr_2O_7$ induced down-regulation of Rgn transcript, starting from 14-week-old groups. The variability within the 38-week group accounted for the lack of statistical difference compared to controls.

The observed effect of $K_2Cr_2O_7$ treatment on the level and significance of change in genes associated with nephrotoxicity suggested a difference in sensitivity with the age for all the four genes. At 6 weeks of age, all changes induced by the treatment were not statistically significant or lower than those induced in the other age groups. Moreover, KIM-1 and Spp1 genes resulted to be more sensitive to drug-induced renal injury in 26- and 38-week-old groups, respectively.

For the other genes, Cln and Rgn, any further difference in sensitivity to $K_2Cr_2O_7$-induced changes was assessed.

4.1.1.2 Histopathology

Histopathology diagnosis revealed that HCBD induced epithelial necrosis/regeneration of tubules located in the outer stripe of the outer cortex and, to lesser extent medullary rays, accounting for the S_3 segment of the proximal tubules (Fig. 19). These changes were observed in 19/20 rats and were mild (1/19 rat), moderate (8/19 rats), or marked (10/19 rats), and not age-related in incidence and severity. In addition, increase in cytoplasmic hyaline droplets was observed in the S1 and S2 segments/*pars convoluta* of the proximal tubules in 4/4 rats at 14 weeks of age. This observation was graded as mild (1/4 rat) to moderate (3/4 rat) and was not associated with features of cellular degeneration.
A single treated rat (no.31), aged 26 weeks, did not show any abnormalities at microscopic examination.

$K_2Cr_2O_7$ induced histopathological changes in the cortical S1 and S2 segments of the proximal tubules in 19/20 treated rats (Fig. 20). These consisted in epithelial vacuolar degeneration/necrosis at 6 weeks of age, which was graded moderate in 3/4 rats or marked in one of them. Starting from 14 weeks of age, marked epithelial necrosis of the same tubular segment was observed in all treated rats. In addition, distally to necrotic segments, tubules were dilated, with scattered apoptotic cells in their lining and tubular lumina were filled by brightly eosinophilic proteinaceous casts and/or cellular debris. Tubular dilation/casts/debris were graded minimal (1/15 rats), mild (5/15 rats), moderate (5/15 rats) or marked (4/15 rats), according to the extension of the damage. Neither tubular epithelium necrosis nor tubular dilation/casts/debris, recorded at 14 weeks of age and over, was age-related in incidence and severity.
A single treated rat (no.53), aged 38 weeks, did not show any abnormalities at microscopic examination.

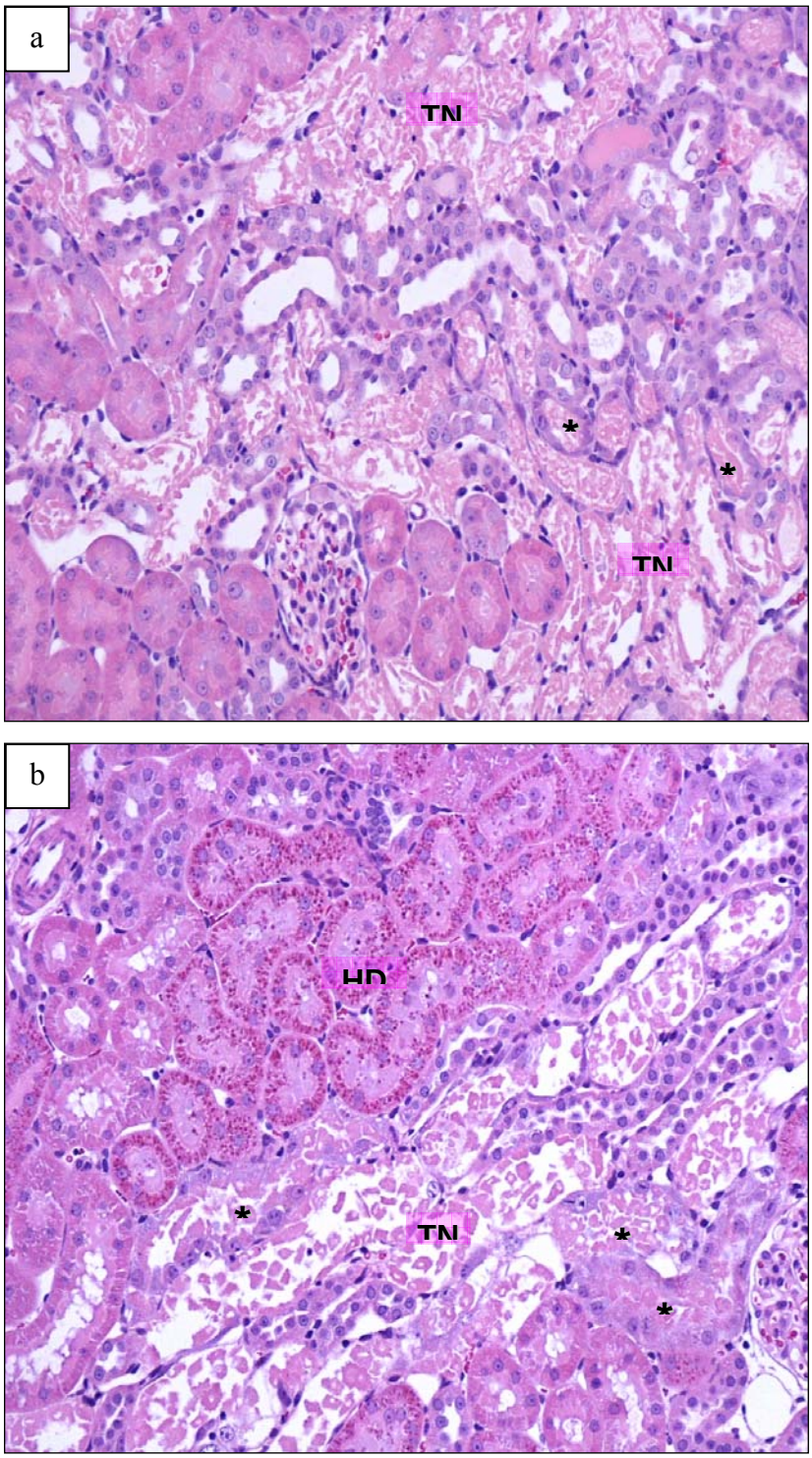

Fig.19 (a-b): Histopathological changes induced by HCBD administration. Necrotic cells (TN) were characterized by hypereosinophilic cytoplasm with loss of nuclear details, detachment from the basement membrane and exfoliation into the lumen. Regenerating tubules (*), characterized by mitotic figures, flattened cells with basophilic cytoplasm and large vesicular nuclei were also present. (b) At 14 weeks of age, increase in round eosinophilic cytoplasmic inclusions (hyaline droplets/HD) were observed in the pars convoluta. H&E 20X. TN: tub. necrosis; *: tub. regeneration; HD: hyaline droplets.

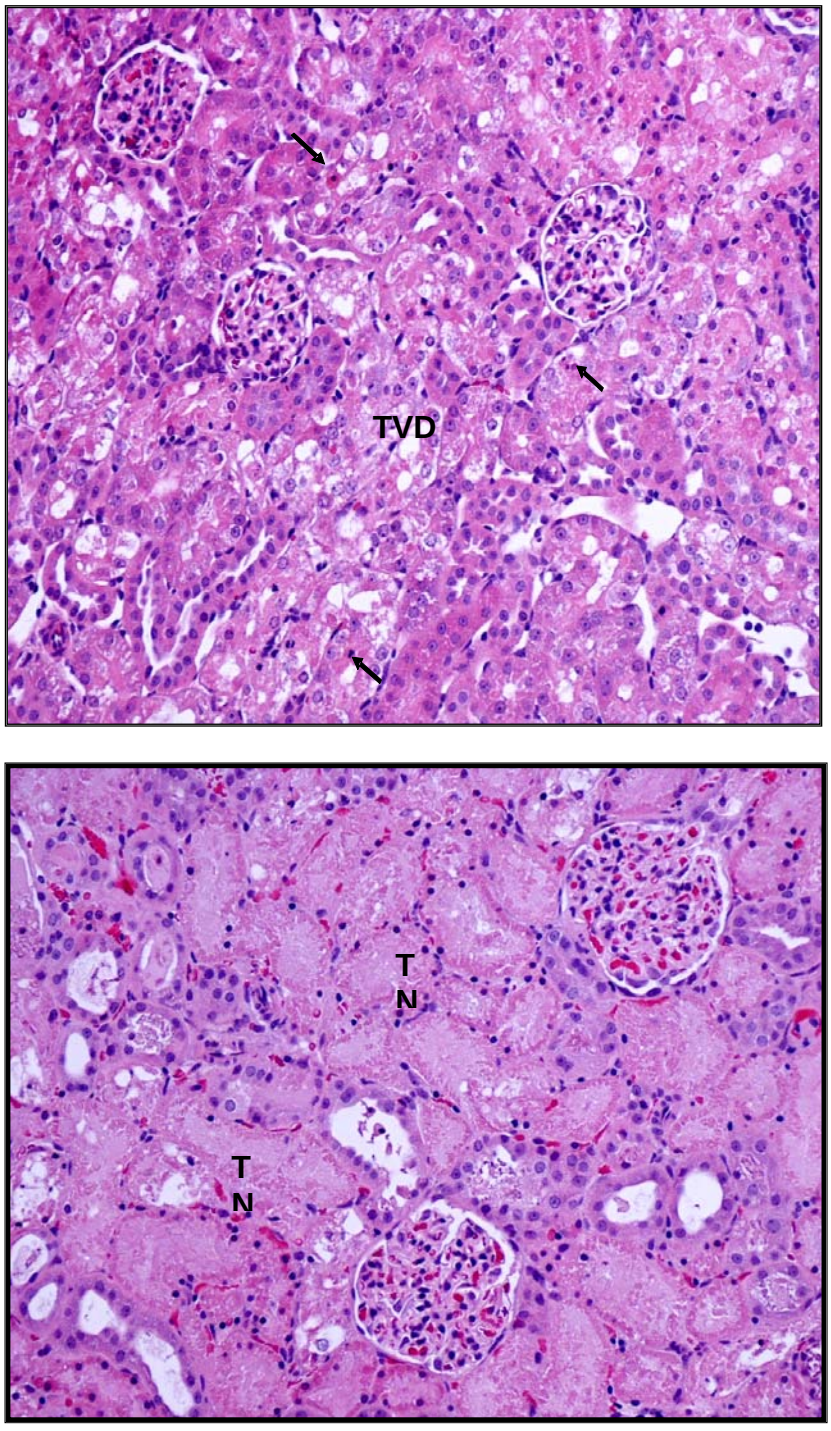

Fig. 20 (a-b): Histopathological changes induced by Potassium dichromate administration. (a) At 6 weeks of age, degenerating epithelial cells showed swollen cytoplasm with clear, irregular-sized vacuoles (TVD). Scattered necrotic/apoptotic cells were also present (arrows). (b) At 14 weeks of age, tubular epithelial cells showed tubular necrosis and were characterized by hypereosinophilic cytoplasm and loss of nuclear details (TN). In addition, distal segments showed dilated lumina, occasionally containing necrotic debris. H&E 20X. TN: tub. necrosis; TVD: tub. vacuolar degeneration; arrows: scattered apoptotic/necrotic cells

4.1.1.3 Clinical chemistry

Treatment with 100 mg/kg HCBD caused increases in plasma urea and creatinine in all groups after 48h from injection (Fig. 21, 22). Whilst increases were statistically significant in all groups of animals for urea, for creatinine the significance was observed in 6-, 14- and 48-week-old groups of animals only.

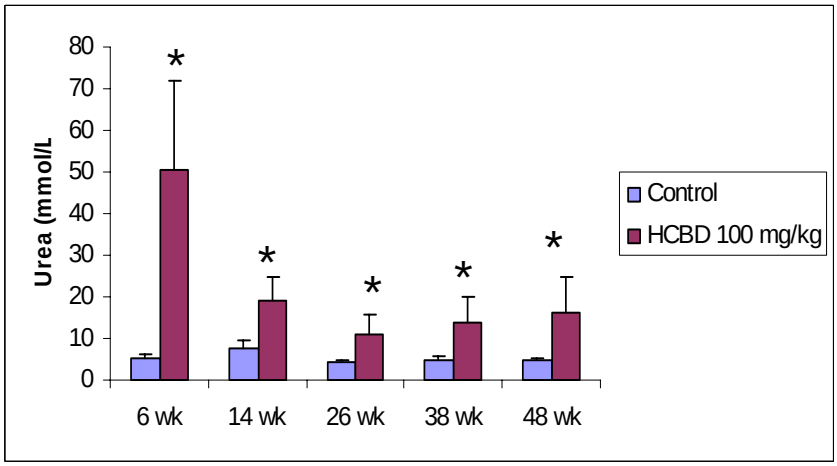

Fig. 21. Change in plasma urea levels following treatment with a single i.p. injection 100 mg/kg HCBD in 6-, -14, -26, -38 or -48-week-old rats. Statistical significance was determined using Dunnett's *t* test (*p < 0.05).

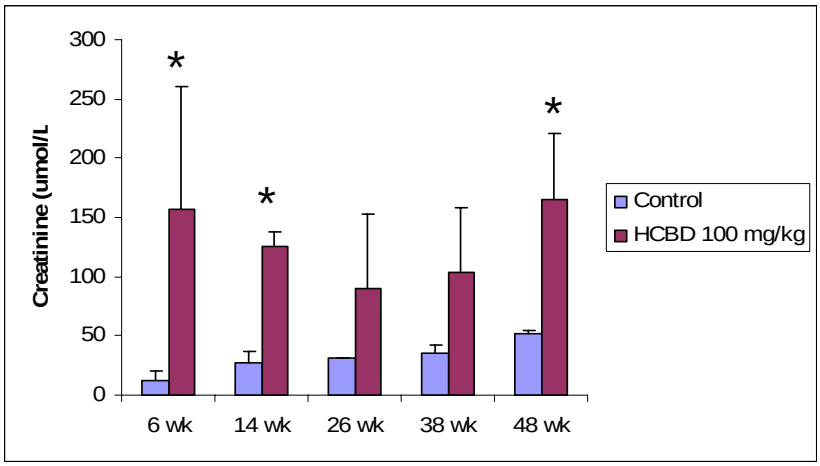

Fig 22. Change in plasma creatinine levels following treatment with a single i.p. injection 100 mg/kg HCBD in 6-, -14, -26, -38 or -48-week-old rats. Statistical significance was determined using Dunnett's *t* test (*p < 0.05).

Treatment with $K_2Cr_2O_7$ 25 mg/kg causes statistically significant increases in plasma urea and creatinine starting from 14-week-old group, higher than increasing caused by HCBD (Fig. 23, 24).

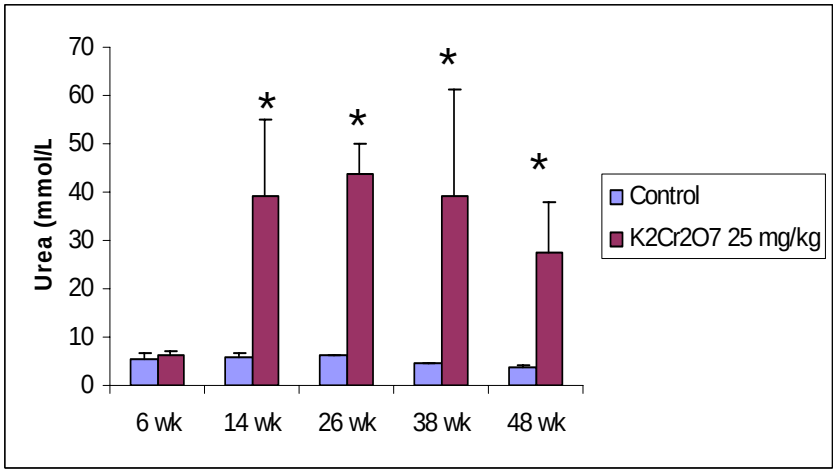

Fig. 23. Change in plasma urea levels following treatment with a single s.c. injection 25 mg/kg $K_2Cr_2O_7$ in 6-, -14, -26, -38 or -48-week-old rats. Statistical significance was determined using Dunnett's *t* test (*p < 0.05).

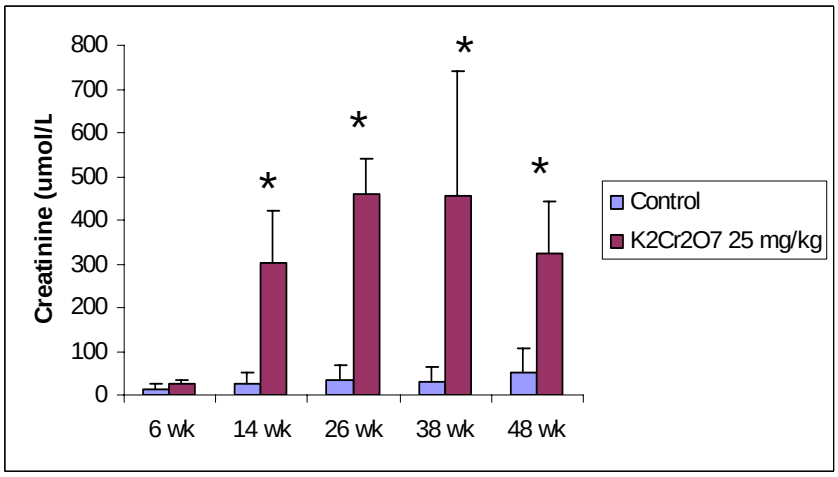

Fig 24. Change in plasma creatinine levels following treatment with a single s.c. injection 25 mg/kg $K_2Cr_2O_7$ in 6-, -14, -26, -38 or -48-week-old rats. Statistical significance was determined using Dunnett's *t* test (*p < 0.05).

4.1.2 Dose-response studies

4.1.2.1 Gene expression

Expression results for all genes, as fold changes, obtained after treatment in 8-week-old rats with a single i.p. injection of HCBD at doses of 25, 50, or 100 mg/kg are reported in Fig. 25.

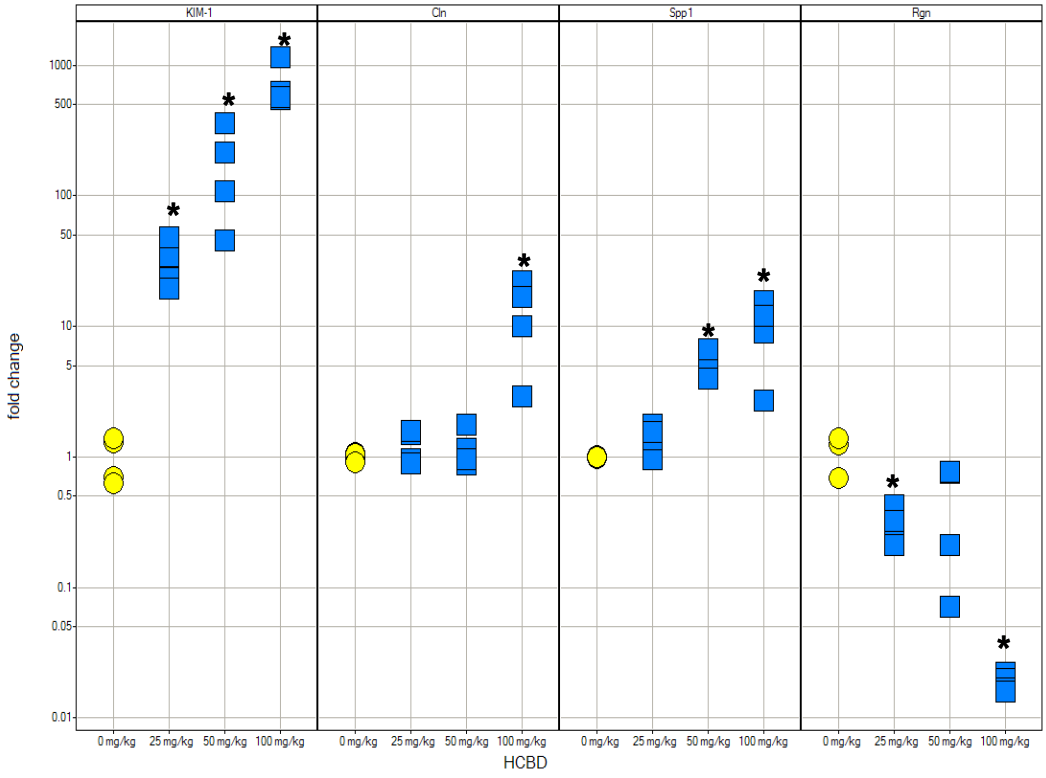

Fig.25. KIM-1, Cln, Spp1, and Rgn mRNA expression (fold change). Transcript levels are shown for individual animals treated with a single i.p. injection of 25, 50, or 100 mg/kg HCBD (blue box, n = 4) relative to average level in controls (vehicle: corn oil, yellow circle, n = 4). Statistical significance in a Student's *t* test comparison of age-matched treated and control values is indicated (*p < 0.05).

Treatment with HCBD caused a significant increase in KIM-1 expression in all groups, up to approximately 700-fold increase of group means over control at 100 mg/kg.

Clusterin mRNA levels were significantly increased (13-fold over control) in the high dose group only.

Spp1 was significantly increased from 5-fold in the 50 mg/kg group up to 10-fold in the 100 mg/kg group.

Rgn transcript levels were decreased by HCBD treatment, and statistical significance was noted in the low and high dose group.

Expression results for all genes, as fold changes, obtained after treatment in 8-week-old rats with a single s.c. injection of $K_2Cr_2O_7$ at doses of 8, 12.5, or 25 mg/kg are reported in Fig. 26.

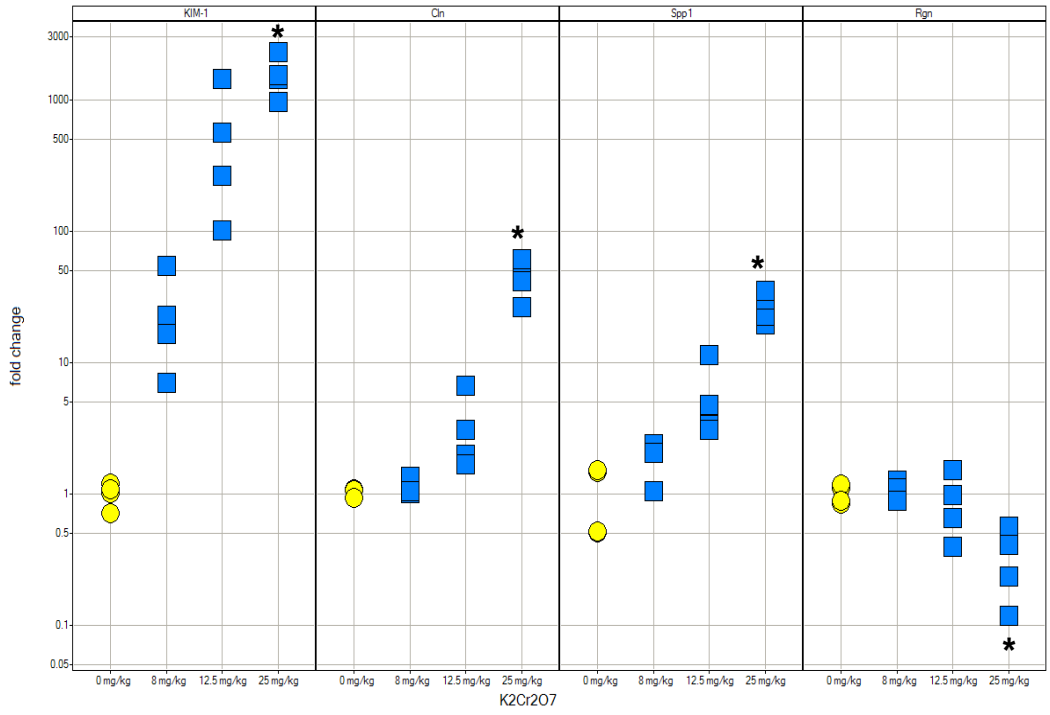

Fig. 26. KIM-1, Cln, Spp1, and Rgn mRNA expression (fold change). Transcript levels are shown for individual animals treated with a single s.c. injection of 8, 12.5, or 25 mg/kg $K_2Cr_2O_7$ (blue box, n = 4) relative to average level in controls (vehicle: corn oil, yellow circle, n = 4). Statistical significance in a Student's *t* test comparison of age-matched treated and control values is indicated (*$p < 0.05$).

Treatment of rats with $K_2Cr_2O_7$ at induced increased expression of KIM-1 in all groups, even if statistically significant in the high dose group only (mean expression of 1600-fold over control). The variability within the other groups accounted for the lack of statistical difference compared to controls, although mean expression in the low and intermediate groups where 25-fold and 600-fold over control). Also in the dose-response studies, $K_2Cr_2O_7$ induced higher expression in KIM-1 gene compared to HCBD.

As observed for HCBD treatment, $K_2Cr_2O_7$ caused significant increased Cln levels (45-fold over control) in the high dose group only, higher than increasing caused by HCBD.

$K_2Cr_2O_7$–induced changes in Spp1 expression were similar to those observed with HCBD, but statistically significant at the high dose only and of greater magnitude (27-fold over control).

Rgn transcript levels were statistically decreased by treatment in the high dose group. Mean expression for this group was 10-fold higher compared to HCBD-induced Rgn expression changes in the same group.

4.1.2.2 Histopathology

Single i.p. injection of HCBD at doses of 100, 50 or 25 mg/kg induced dose-related histopathological finding in rats aged 8 weeks. At 100 mg/kg, 4/4 rats were affected by marked tubular necrosis/regeneration of the S3 segment/*pars recta* of proximal tubules. In 3 of these rats, this observation was associated with increase in cytoplasmic hyaline droplets in the S1 and S2 segments and graded mild (1/3) or moderate in 2 of them. At 50 mg/kg, tubular necrosis/regeneration was still present in 4/4 rats but appeared less severe, being minimal (3/4 rats) or mild (1/4). At 25 mg/kg, tubules of the S3 segment/*pars recta* were unaffected in all rat, while cytoplasmic hyaline droplets were mildly increased in 3/4 rats.

Single s.c. injection of $K_2Cr_2O_7$ at doses of 25, 12.5 and 8 mg/kg induced dose-related histopathological finding in rats aged 8 weeks. At 25 mg/kg, 4/4 rats showed marked tubular necrosis of the S1/S2 segments of the proximal tubules. In addition, tubular dilation with single cell degeneration and intratubular casts/cellular debris was recorded for all these rats and was minimal (3/4 rats) to mild (1/4 rat). At 12.5 mg/kg, tubular vacuolar degeneration/necrosis was minimal in 1/4 rat, affecting only single cells within tubular lining, or moderate 2/4 rats. In these two, regenerating cells (mitotic figures/basophilic cells with prominent nuclei/nucleoli) were detected, admixed to those undergoing degeneration/necrosis. At 8 mg/kg, regeneration (increased mitotic figures),

without clear evidences of tubular cell necrosis, were seen in 2/4 rats, affecting a minimal number of tubules.

4.1.2.3 Clinical chemistry

Treatment with different doses of HCBD in animals at 8 weeks of age caused statistical significant increase in plasma urea and creatinine levels in the high dose group (100 mg/kg) (Fig. 27, 28).

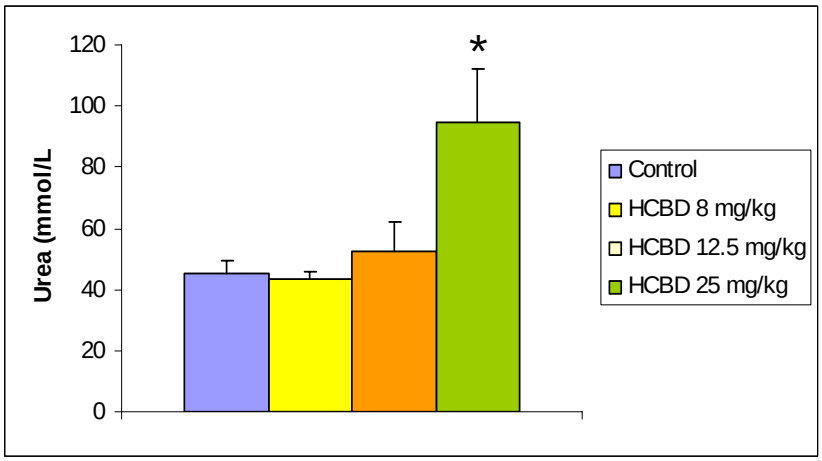

Fig. 27. Change in plasma urea levels following treatment with a single i.p. injection HCBD (25, 50 or 100 mg/kg) in 8-week-old rats. Statistical significance was determined using Dunnett's *t* test (*p < 0.05).

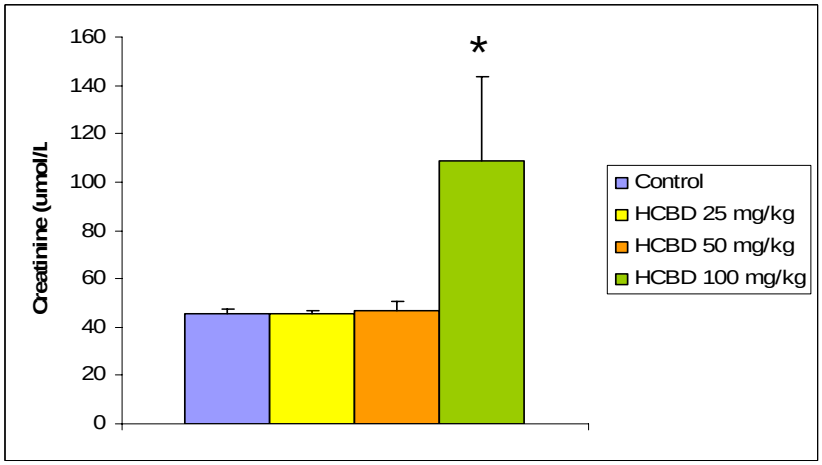

Fig. 28. Change in plasma creatinine levels following treatment with a single i.p. injection HCBD (25, 50 or 100 mg/kg) in 8-week-old rats. Statistical significance was determined using Dunnett's *t* test (*p < 0.05).

Treatment with different doses of $K_2Cr_2O_7$ in 8-week-old animals showed statistical significant increase in plasma creatinine and urea levels in the high dose group (25 mg/kg) (Fig. 29, 30). While the increase in plasma levels of creatinine were similar to HCBD, for urea the increase $K_2Cr_2O_7$-induced was lower than HCBD.

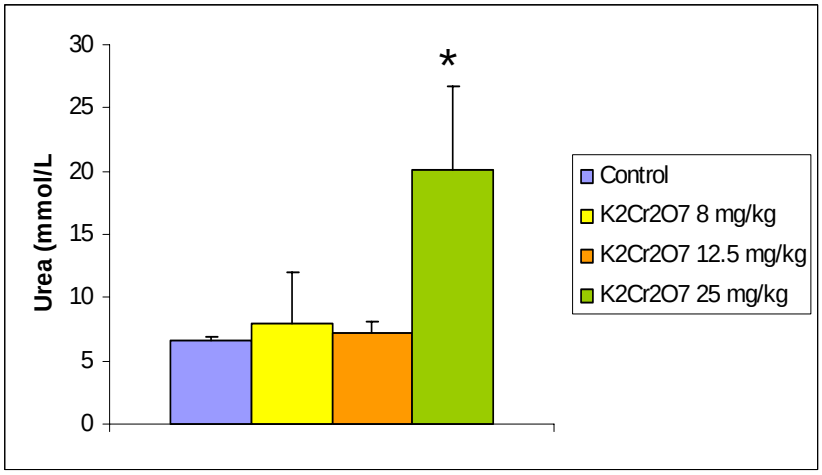

Fig. 30. Change in plasma urea levels following treatment with a single s.c. injection $K_2Cr_2O_7$ (8, 12.5 or 25 mg/kg) in 8-week-old rats. Statistical significance was determined using Dunnett's *t* test (*p < 0.05).

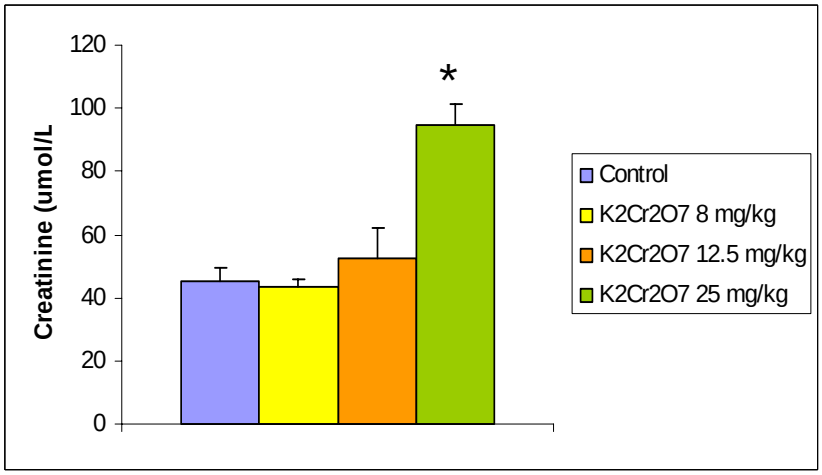

Fig. 31. Change in plasma creatinine levels following treatment with a single s.c. injection $K_2Cr_2O_7$ (8, 12.5 or 25 mg/kg) in 8-week-old rats. Statistical significance was determined using Dunnett's *t* test (*p < 0.05).

4.2 Phase II

4.2.1 Dose-response Cephaloridine study

4.2.1.1 Gene expression

The dose-dependent effects of Cephaloridine (250, 500, or 1000 mg/kg) on the four putative gene expression markers of nephrotoxicity were assessed (Fig. 32).

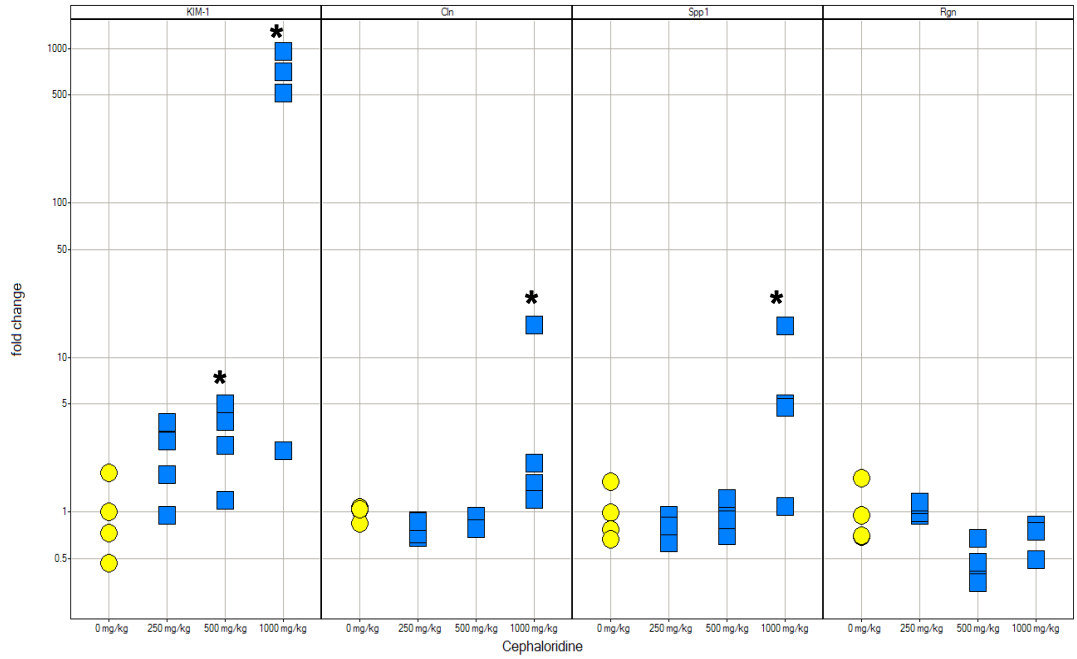

Fig. 32. KIM-1, Cln, Spp1, and Rgn mRNA expression (fold change). Transcript levels are shown for individual animals treated with a single i.p. injection of 250, 500, or 1000 mg/kg Cephaloridine (blue box, n = 4) relative to average level in controls (vehicle: corn oil, yellow circle, n = 4). Statistical significance in a Student's *t* test comparison of age-matched treated and control values is indicated (*p < 0.05).

KIM-1 mRNA levels were significantly increased starting from 500 mg/kg to high dose group, up to 540-fold over control.

Cln expression was increased (5-fold over control) by Cephaloridine at 1000 mg/kg.

Spp1 was observed to have expression patterns induced by Cephaloridine similar to Cln, showing increased mRNA levels (7-fold over control) in the high dose group.

No statistically and biologically significant changes were observed for Rgn expression levels in all Cephaloridine treatment groups.

4.2.1.2 Histopathology

Single i.p. injection of Cephaloridine at doses of 1000, 500 or 250 mg/kg induced histopathological finding in 8-week-old rats at 1000 mg/kg (Fig. 33). These consisted in tubular necrosis of the S2 segments of the proximal tubules with relative sparing of the S1 portion. Tubular necrosis was seen in 3/4 rats and graded mild in one rat or marked in two. In one of the rats severely affected, the damage started extending to the S3 portion of the proximal tubules.

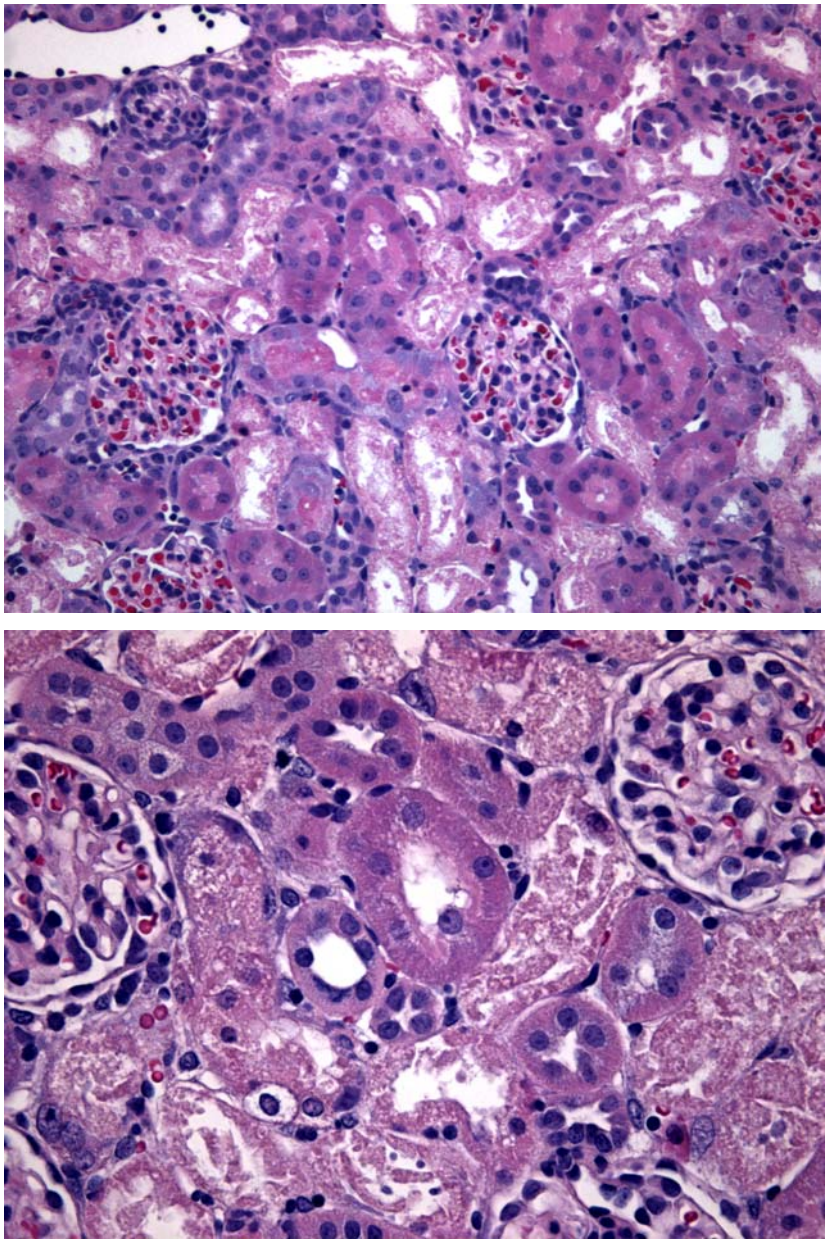

Fig 33: Histopathological changes induced by Cephaloridine administration, consisting in tubular necrosis the proximal tubules with relative sparing of those in close proximity to the renal corpuscles, likely to represent the S1 portion. Few regenerating tubules were also present.

4.2.1.3 Clinical chemistry

Treatment of 8-week-old rats with a single i.p. injection of 250, 500 or 1000 mg/kg Cephaloridine showed no significant changes in plasma urea and creatinine levels after 48h from treatment (Fig. 33, 34).

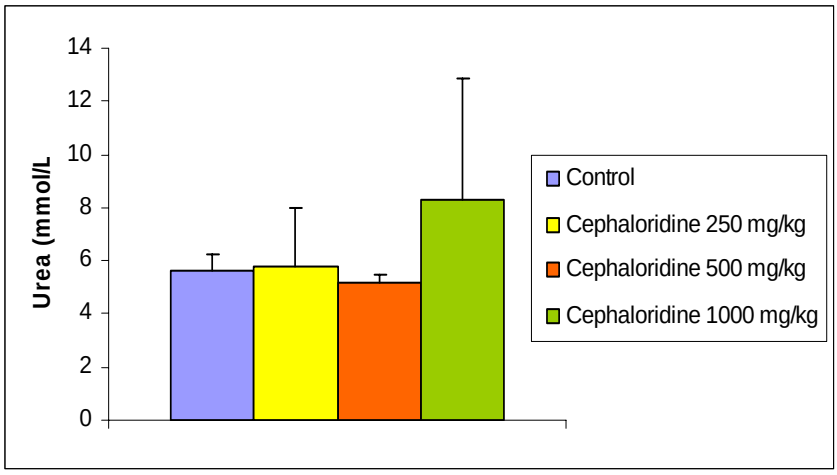

Fig. 33. Change in plasma urea levels following treatment with a single i.p. injection Cephaloridine (250, 500 or 1000 mg/kg) in 8-week-old rats. Statistical significance was determined using Dunnett's *t* test (*p < 0.05).

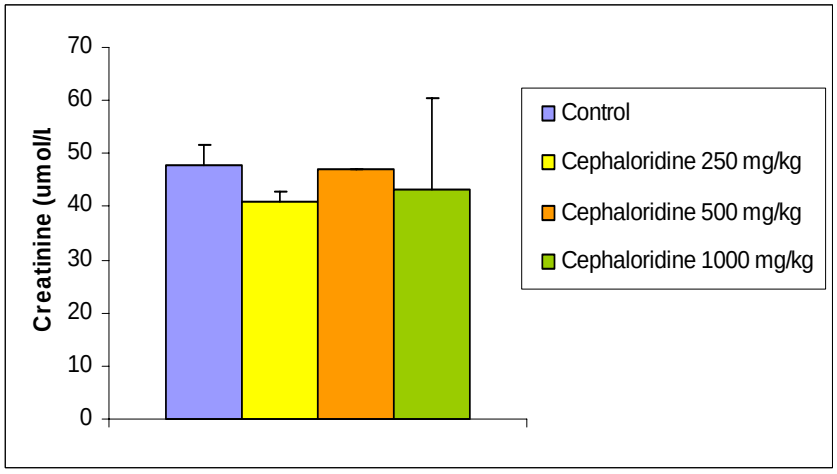

Fig. 34. Change in plasma creatinine levels following treatment with a single i.p. injection Cephaloridine (250, 500 or 1000 mg/kg) in 8-week-old rats. Statistical significance was determined using Dunnett's *t* test (*p < 0.05).

5 DISCUSSION

The identification and evaluation of novel biomarkers of target organ toxicity has been one of the main applications of genomic-based technologies (Fielden and Zacharewski, 2001; Goodsaid, 2003; Huang et al., 2001 and Storck et al., 2002). A common approach in the literature has been to use cDNA or oligo microarrays for the classification of xenobiotics based on their gene expression profiles.

One area in which this approach has been recently applied is drug-induced nephrotoxicity in rodents. Many of published literature employed cDNA arrays to assess known xenobiotic-induced nephrotoxicity in rats (Huang et al., 2001). Gene expression changes were observed in a multitude of distinct pathways. Some of these are involved in tissue damage, remodelling and regeneration, disruption of calcium homeostasis, oxidative stress. Many of these reports detail cellular pathways that are modulated through the course of lesion development.

Signature of genes designed to indicate nephrotoxicity obtained by microarray technology need to be validated with an independent gene expression detection technology such as quantitative reverse transcriptase-polymerase chain reaction (qRT-PCR).

On the basis of published works, four genes were selected for evaluation in a rodent model of nephrotoxicity. All the selected genes correlate with known functional changes in response to drug-induced kidney injury.

KIM-1, which encodes a type I cell membrane glycoprotein, was cloned from post-ischemic rat kidneys. As with clusterin and OPN, expression of KIM-1 is thought to be associated with de-differentiated tubular epithelial cells, although a role in cellular regeneration has not been established. During this process, the ectodomain of KIM-1 is shed into the lumen and excreted in the urine. Because the upregulation of KIM-1 occurs rapidly and is detected in the urine, it has been proposed as an accessible biomarker of renal proximal tubular damage in humans (Han et al., 2002).

Clusterin, also known as sulfated glycoprotein-2 (SGP-2), is a ubiquitously expressed glycoprotein whose expression in the kidney is upregulated during

development, in response to drug-induced cortical tubular injury, as well as in a variety of renal diseases and toxicities (Correa-Rotter et al., 1998; Darby et al., 1995; Dvergsten et al., 1994; Laping et al., 1997; Rosenberg and Silkensen, 1995; Schwochau et al., 1998 and Silkensen et al., 1997). Urinary clusterin excretion is detectable before serum creatinine changes (Aulitzky et al., 1992 and Eti et al., 1993). The exact role clusterin plays in renal injury is not well understood. Because clusterin is able to induce cell aggregation for several cell types in vitro, its induction and active secretion by stressed cells during injury or remodeling have been hypothesized (Silkensen et al., 1995). In this scenario, clusterin would act as a "bridge" to keep cells in close proximity to allow for specific cell–cell interactions and signalling to occur.

Increased expression of Spp1 has also been demonstrated in numerous rodent models of renal injury, not just those involving proximal tubular necrosis. In rats treated with high doses of gentamicin, Spp1 mRNA was detected in regenerating proximal tubules, proliferating cortical distal tubules, and medullary tubules (Verstrepen et al., 2001 and Xie et al., 2001). Two divergent roles for Spp1 have been proposed during the development of acute renal failure. It may be involved in macrophage infiltration that occurs in response to glomerulnephritis (Wuthrich et al., 1998). It also protects cells from ischemic injury in gentamicin-treated rats by inhibiting apoptosis through decreased inducible nitric oxide synthase (iNOS) expression (Noiri et al., 1999). Unlike clusterin, increased urinary osteopontin excretion has not been observed in response to renal damage; however, it has been shown to decrease in the urine of patients with primary glomerulonephritis (Gang et al., 2001). Under normal conditions, Spp1 is secreted in the urine where it acts to prevent calcium oxalate crystal aggregation and stone formation (Min et al., 1998).

Regucalcin, is the Ca^{2+}-binding protein, and it plays an important role in the regulation of kidney cell functions related to Ca^{2+}. In particular, regucalcin has an important role in the reabsorption of Ca^{2+} in the kidney cortex. Presumably, regucalcin is responsible for ATP-dependent transcellular Ca^{2+} transport, and it participates in the promotion of Ca^{2+} reabsorption in the nephron tubulo of kidney

cortex. Kidney regucalcin may play a physiological role in the regulation of calcium metabolism in blood through reabsorption of urinary calcium.

Cell damage induced by nephrotoxicants (i.e., cisplatin) can induce significant changes in Rgn due to disruption of Ca^{2+} homeostasis (Chao, 1996 and Kurota and Yamaguchi, 1995),

In this work of thesis the four selected genes were evaluated in male rats after treatment with HCBD, $K_2Cr_2O_7$, and Cephaloridine, three nephrotoxicants that primarily injure specific regions of the proximal tubule via different mechanisms of action.

In the first part of the experimental phase (validation), transcript levels of KIM-1, Cln, Spp-1, and Rgn were quantified after treatment with a single dose of HCBD, $K_2Cr_2O_7$ in rats at different ages. The aim of this experiment was to investigate changes in genes identified as markers of drug-induced renal damage in rodents.

Expression changes correlated with the appearance of segment-specific renal lesion caused by the two compounds. In particular, HCBD (100 mg/kg) treatment induced epithelial necrosis/regeneration of the S3 segment/*pars recta* of proximal tubules, not age-related in incidence and severity. High levels of plasma creatinine and urea were detectable in all HCBD treatment groups, indicating functional disruption of kidney. All the selected genes showed significant changes in expression after treatment with HCBD in all groups. One rat did not show any abnormalities at microscopic examination and clinical chemistry analysis although at gene expression evaluation significant increases were observed in the same animal for KIM-1 levels.

Treatment with a single dose of $K_2Cr_2O_7$ (25 mg/kg) induced histopathological changes in the cortical S1 and S2 segments of the proximal tubules in treated rats. Morphological changes at 6-weeks were indicative of an early damage of tubular cells (degeneration/necrosis), while starting from the 14-week-old groups of animals the damage appeared already established (necrosis). The different level of damage induced by $K_2Cr_2O_7$ was captured by gene expression analysis. In fact, within the panels of genes evaluated, KIM-1 only showed a significant increase at 6 weeks of age. No significant alterations in plasmatic creatinine and urea were

assessed in the 6-week-old group. One rat did not show any abnormalities at microscopic examination, clinical chemistry analysis and gene expression evaluation.

In the second part of low-scale validation phase, three different doses of HCBD and $K_2Cr_2O_7$, including the high dose used in the ageing study, were selected and somministered to 8-week-old rats to monitor the progression/severity of compound-induced damage and its effect on traditional and genomic markers.

Treatment with 25, 50, or 100 mg/kg HCBD and 8, 12.5, or 25 mg/kg $K_2Cr_2O_7$ in animals at 8 weeks of age resulted in the same histopathologic, clinical chemistry and gene expression modifications assessed in the previous ageing study for the high dose groups (100 and 25 mg/kg, respectively).

At intermediate dose with both nephrotoxicants, the same morphologic findings related with specific compound toxicity (S3 segment tubular necrosis/regeneration for HCBD and S1-S2 segments degeneration/necrosis for $K_2Cr_2O_7$) were still present but showed a lower degree of severity. Moreover, at 8 mg/kg degeneration necrosis affected single cell (rather than the entire epithelium) in one animal only while an increase of mitotic figures in a minimal number of tubules was seen in 2 animals. This observation was likely to represent the reparative process to a previous insult. The low severity of microscopic observations was captured by gene expression response. In particular, KIM-1 and Spp1 genes showed statistically significant increased levels in animals treated with intermediate dose and KIM-1 mRNA transcript only was significantly increased at low dose of both nephrotoxicants.

On the contrary, clinical chemistry markers did not show any changes in plasma concentrations at the intermediate and low doses of HCBD or $K_2Cr_2O_7$.

Treatment of 8-week-old rats with a single injection of different doses of Cephaloridine (250, 500, or 1000 mg/kg) induced morphological findings (S2 segment tubular necrosis) in three animals from the high dose group only. No changes in creatinine and urea plasmatic levels were observed in all the treated groups.

At gene expression, KIM-1, Cln and Spp1 showed increases at high dose, although the increase was statistically significant for KIM-1 only. This was due to

the high variability of the high dose group given by an outlier animal that did not show any change at microscopic examination, clinical chemistry analysis and gene expression evaluation. Moreover, KIM-1 mRNA levels were statistically significantly increased also at 500 mg/kg, where no modifications were seen at histopathology and clinical chemistry analysis.

In summary, genes whose expressions have been previously correlated with drug-induced renal injury in rodents were evaluated using segment-specifictoxic compounds for the proximal tubule. Microscopic damage in proximal tubules reflected the severity of the insult, with marked necrosis being observed at the high doses. Lower doses induced less severe necrosis and/or degeneration. Plasmatic levels of traditional clinical markers for renal damage, urea and creatinine, did not correlate well with the microscopic alterations observed. In fact, changes were detected only at high doses, after a significant damage to nephrons has already occurred, thus resulting not very sensitive. Tubular damage and severity evidenced in these experiments were correlated with gene changes. Commensurate with the damage, epithelial necrosis was associated with a greater abundance of gene expression changes. Interestingly, even low severity microscopic observations were evidenced by gene expression quantification. Our analysis suggested at least equal sensitivity of gene expression quantification by qRT-PCR technology compared to traditional morphological endpoints.

This study suggested also KIM-1 as specific marker of tubular injury, which could provide a more sensitive indication of damage compared with traditional clinical measurements. Moreover, since its increased expression was evidenced also for low dose of nephrotoxicants where no morphologic modifications were observed, KIM-1 is likely to represent a potential predictive biomarker of nephrotoxicity.

In conclusion, this study confirmed that gene expression quantification may be used to detect renal tubular damage induced by nephrotoxicants. Genomic responses could represent more sensitive tool to monitor renal damage in comparison with traditional morphological and biochemical end points.

6 REFERENCE LIST

(1) Amin RP, Vickers AE, Sistare F et al. Identification of putative gene based markers of renal toxicity. Environ Health Perspect 2004 March;112(4):465-79.

(2) Appenroth D, Winnefeld K. Vitamin E and C in the prevention of metal nephrotoxicity in developing rats. Exp Toxicol Pathol 1998 September;50(4-6):391-6.

(3) Bagchi D, Ray SD, Bagchi M et al. Mechanistic pathways of antioxidant cytoprotection by a novel IH636 grape seed proanthocyanidin extract. Indian J Exp Biol 2002 June;40(6):717-26.

(4) Barclay TB, Peters JM, Sewer MB et al. Modulation of cytochrome P-450 gene expression in endotoxemic mice is tissue specific and peroxisome proliferator-activated receptor-alpha dependent. J Pharmacol Exp Ther 1999 September;290(3):1250-7.

(5) Barrera D, Maldonado PD, Medina-Campos ON et al. Protective effect of SnCl2 on K2Cr2O7-induced nephrotoxicity in rats: the indispensability of HO-1 preinduction and lack of association with some antioxidant enzymes. Life Sci 2003 October 24;73(23):3027-41.

(6) Barrera D, Maldonado PD, Medina-Campos ON et al. HO-1 induction attenuates renal damage and oxidative stress induced by K2Cr2O7. Free Radic Biol Med 2003 June 1;34(11):1390-8.

(7) Bello-Klein A, Bock PM, Travacio M et al. Myocardial oxidative stress and antioxidants in hypertension as a result of nitric oxide synthase inhibition. Cardiovasc Toxicol 2001;1(1):43-50.

(8) Bennett WM. Cyclosporine nephrotoxicity: implications for dermatology. Int J Dermatol 1997 December;36 Suppl 1:11-4.

(9) Birner G, Bernauer U, Werner M, Dekant W. Biotransformation, excretion and nephrotoxicity of haloalkene-derived cysteine S-conjugates. Arch Toxicol 1997;72(1):1-8.

(10) Boring L, Gosling J, Monteclaro FS et al. Molecular cloning and functional expression of murine JE (monocyte chemoattractant protein 1) and murine macrophage inflammatory protein 1alpha receptors: evidence for two closely linked C-C chemokine receptors on chromosome 9. J Biol Chem 1996 March 29;271(13):7551-8.

(11) Boroushaki MT. Development of resistance against hexachlorobutadiene in the proximal tubules of young male rat. Comp Biochem Physiol C Toxicol Pharmacol 2003 December;136(4):367-75.

(12) Burch HB, Chan AW, Alvey TR, Lowry OH. Localization of glutamine accumulation and tubular reabsorption in rat nephron. Kidney Int 1978 November;14(5):406-13.

(13) Burch HB, Choi S, McCarthy WZ et al. The location of glutamine synthetase within the rat and rabbit nephron. Biochem Biophys Res Commun 1978 May 30;82(2):498-505.

(14) Burch HB, Narins RG, Chu C et al. Distribution along the rat nephron of three enzymes of gluconeogenesis in acidosis and starvation. Am J Physiol 1978 September;235(3):F246-F253.

(15) Cristofori P, Zanetti E, Fregona D et al. Renal proximal tubule segment-specific nephrotoxicity: an overview on biomarkers and histopathology. Toxicol Pathol 2007;35(2):270-5.

(16) Denhardt DT, Guo X. Osteopontin: a protein with diverse functions. FASEB J 1993 December;7(15):1475-82.

(17) Denhardt DT, Feng B, Edwards DR et al. Tissue inhibitor of metalloproteinases (TIMP, aka EPA): structure, control of expression and biological functions. Pharmacol Ther 1993 September;59(3):329-41.

(18) Dobyan DC, Bulger RE. Partial protection by chlorpromazine in mercuric chloride-induced acute renal failure in rats. Lab Invest 1984 May;50(5):578-86.

(19) Duarte CG, Zhang J, Ellis S. Effects of radiocontrast, mannitol, and endothelin on blood pressure and renal damage in the aging male spontaneously hypertensive rat. Invest Radiol 1999 July;34(7):455-62.

(20) Duarte ME, Peixoto AL, Pacheco A, Jorgetti V. [Mast cell hyperplasia in bone oxalosis]. Rev Assoc Med Bras 1999 April;45(2):95-8.

(21) Eknoyan G, Qunibi WY, Grissom RT et al. Renal papillary necrosis: an update. Medicine (Baltimore) 1982 March;61(2):55-73.

(22) Eknoyan G, Bulger RE, Dobyan DC. Mercuric chloride-induced acute renal failure in the rat. I. Correlation of functional and morphologic changes and their modification by clonidine. Lab Invest 1982 June;46(6):613-20.

(23) Evan AP, Dail WG, Jr. The effects of sodium chromate on the proximal tubules of the rat kidney. Fine structural damage and lysozymuria. Lab Invest 1974 June;30(6):704-15.

(24) Gibey R, Dupond JL, Alber D et al. Predictive value of urinary N-acetyl-beta-D-glucosaminidase (NAG), alanine-aminopeptidase (AAP) and beta-2-microglobulin (beta 2M) in evaluating nephrotoxicity of gentamicin. Clin Chim Acta 1981 October 8;116(1):25-34.

(25) Gong X, Shang F, Obin M et al. Antioxidant enzyme activities in lens, liver and kidney of calorie restricted Emory mice. Mech Ageing Dev 1997 December 30;99(3):181-92.

(26) Guder WG, Ross BD. Enzyme distribution along the nephron. Kidney Int 1984 August;26(2):101-11.

(27) Guder WG, Purschel S, Vandewalle A, Wirthensohn G. Bioluminescence procedures for the measurement of NAD(P) dependent enzyme catalytic activities in submicrogram quantities of rabbit and human nephron structures. J Clin Chem Clin Biochem 1984 February;22(2):129-40.

(28) Hassoun EA, Stohs SJ. Chromium-induced production of reactive oxygen species, DNA single-strand breaks, nitric oxide production, and lactate dehydrogenase leakage in J774A.1 cell cultures. J Biochem Toxicol 1995 December;10(6):315-21.

(29) Hubank M, Mayne L. Expression of the excision repair gene, ERCC3 (excision repair cross-complementing), during mouse development. Brain Res Dev Brain Res 1994 August 12;81(1):66-76.

(30) Hubank M, Schatz DG. Identifying differences in mRNA expression by representational difference analysis of cDNA. Nucleic Acids Res 1994 December 25;22(25):5640-8.

(31) Ichimura T, Bonventre JV, Bailly V et al. Kidney injury molecule-1 (KIM-1), a putative epithelial cell adhesion molecule containing a novel immunoglobulin domain, is up-regulated in renal cells after injury. J Biol Chem 1998 February 13;273(7):4135-42.

(32) Iida K, Shinki T, Yamaguchi A et al. A possible role of vitamin D receptors in regulating vitamin D activation in the kidney. Proc Natl Acad Sci U S A 1995 June 20;92(13):6112-6.

(33) Iqbal K, Ottaway JH. Glutamine synthetase in muscle and kidney. Biochem J 1970 September;119(2):145-56.

(34) Ishmael J, Pratt I, Lock EA. Necrosis of the pars recta (S3 segment) of the rat kidney produced by hexachloro 1:3 butadiene. J Pathol 1982 October;138(2):99-113.

(35) Jentoft N. Why are proteins O-glycosylated? Trends Biochem Sci 1990 August;15(8):291-4.

(36) Jose PA, Yu PY, Yamaguchi I et al. Dopamine D1 receptor regulation of phospholipase C. Hypertens Res 1995 June;18 Suppl 1:S39-S42.

(37) Khan SR, Johnson JM, Peck AB et al. Expression of osteopontin in rat kidneys: induction during ethylene glycol induced calcium oxalate nephrolithiasis. J Urol 2002 September;168(3):1173-81.

(38) Kilty C, Doyle S, Hassett B, Manning F. Glutathione S-transferases as biomarkers of organ damage: applications of rodent and canine GST enzyme immunoassays. Chem Biol Interact 1998 April 24;111-112:123-35.

(39) Kurota H, Yamaguchi M. Suppressed expression of calcium-binding protein regucalcin mRNA in the renal cortex of rats with chemically induced kidney damage. Mol Cell Biochem 1995 October 4;151(1):55-60.

(40) Laterza OF, Hansen WR, Taylor L, Curthoys NP. Identification of an mRNA-binding protein and the specific elements that may mediate the pH-responsive induction of renal glutaminase mRNA. J Biol Chem 1997 September 5;272(36):22481-8.

(41) Lieske JC, Walsh-Reitz MM, Toback FG. Calcium oxalate monohydrate crystals are endocytosed by renal epithelial cells and induce proliferation. Am J Physiol 1992 April;262(4 Pt 2):F622-F630.

(42) Liu H, Bowes RC, III, van de WB et al. Endoplasmic reticulum chaperones GRP78 and calreticulin prevent oxidative stress, Ca2+ disturbances, and cell death in renal epithelial cells. J Biol Chem 1997 August 29;272(35):21751-9.

(43) Lock EA, Ishmael J, Pratt I. Hydropic change in rat liver induced by hexachloro-1:3-butadiene. J Appl Toxicol 1982 December;2(6):315-20.

(44) Lopez CA, Hoyer JR, Wilson PD et al. Heterogeneity of osteopontin expression among nephrons in mouse kidneys and enhanced expression in sclerotic glomeruli. Lab Invest 1993 September;69(3):355-63.

(45) Naidu SG, Lee FT, Jr. Contrast nephrotoxicity: predictive value of urinary enzyme markers in a rat model. Acad Radiol 1994 September;1(1):3-9.

(46) O'Brien C. Lucky break for kidney disease gene. Science 1994 June 24;264(5167):1844.

(47) O'Brien JA, Van Why SK, Keller MS et al. Altered renovascular resistance after spontaneous recovery from hemolytic uremic syndrome. Yale J Biol Med 1994 January;67(1-2):1-14.

(48) Odinecs A, Maso S, Nicoletto G et al. Mechanism of sex-related differences in nephrotoxicity of 1.2-dichloropropane in rats. Ren Fail 1995 September;17(5):517-24.

(49) Pedraza-Chaverri J, Barrera D, Medina-Campos ON et al. Time course study of oxidative and nitrosative stress and antioxidant enzymes in K2Cr2O7-induced nephrotoxicity. BMC Nephrol 2005;6(1):4.

(50) Pedraza-Chaverri J, Murali NS, Croatt AJ et al. Proteinuria as a determinant of renal expression of heme oxygenase-1: studies in models of glomerular and tubular proteinuria in the rat. Am J Physiol Renal Physiol 2006 January;290(1):F196-F204.

(51) Price RG. Urinary enzymes, nephrotoxicity and renal disease. Toxicology 1982;23(2-3):99-134.

(52) Rosenberg ME, Silkensen J. Clusterin: physiologic and pathophysiologic considerations. Int J Biochem Cell Biol 1995 July;27(7):633-45.

(53) Rosenberg ME, Silkensen J. Clusterin and the kidney. Exp Nephrol 1995 January;3(1):9-14.

(54) rreola-Mendoza L, Reyes JL, Melendez E et al. Alpha-tocopherol protects against the renal damage caused by potassium dichromate. Toxicology 2006 February 1;218(2-3):237-46.

(55) Scherberich J, Tuengerthal S, Kollath J. Monitoring of contrast media nephrotoxicity by specific kidney tissue proteinuria of membrane antigens. Fortschr Geb Rontgenstrahlen Nuklearmed Erganzungsbd 1983;118:37-42.

(56) Scherberich JE, Mondorf WA. [Assessment of drug nephrotoxicity by the excretion of tubule-specific membrane antigens and enzymes]. Z Gesamte Inn Med 1983 November 1;38(21):571-80.

(57) Sheridan AM, Bonventre JV. Cell biology and molecular mechanisms of injury in ischemic acute renal failure. Curr Opin Nephrol Hypertens 2000 July;9(4):427-34.

(58) Shi SJ, Rakugi H, Higashimori K et al. Augmentation of angiotensin II release from isolated mesenteric arteries of Wistar-Kyoto and spontaneously hypertensive rats following nephrectomy. Clin Exp Pharmacol Physiol 1994 October;21(10):767-73.

(59) Shi SJ, Rakugi H, Higashimori K et al. Activated angiotensin II generation and regulation in rat mesenteric arteries following nephrectomy. Blood Press Suppl 1994;5:27-31.

(60) Shi ZM, Feng P, Jiang DQ, Wang XJ. Mistletoe alkali inhibits peroxidation in rat liver and kidney. World J Gastroenterol 2006 July 7;12(25):4052-5.

(61) Shimokawa N, Isogai M, Yamaguchi M. Specific species and tissue differences for the gene expression of calcium-binding protein regucalcin. Mol Cell Biochem 1995 February 9;143(1):67-71.

(62) Silkensen JR, Skubitz KM, Skubitz AP et al. Clusterin promotes the aggregation and adhesion of renal porcine epithelial cells. J Clin Invest 1995 December;96(6):2646-53.

(63) Silverblatt F, Turck M, Bulger R. Nephrotoxicity due to cephaloridine: a light- and electron-microscopic study in rabbits. J Infect Dis 1970 July;122(1):33-44.

(64) Squibb KS, Ridlington JW, Carmichael NG, Fowler BA. Early cellular effects of circulating cadmium-thionein on kidney proximal tubules. Environ Health Perspect 1979 February;28:287-96.

(65) Stohs SJ, Bagchi D. Oxidative mechanisms in the toxicity of metal ions. Free Radic Biol Med 1995 February;18(2):321-36.

(66) Stohs SJ. The role of free radicals in toxicity and disease. J Basic Clin Physiol Pharmacol 1995;6(3-4):205-28.

(67) Taylor SA, Chivers ID, Price RG et al. The assessment of biomarkers to detect nephrotoxicity using an integrated database. Environ Res 1997 October;75(1):23-33.

(68) Thadhani R, Pascual M, Bonventre JV. Acute renal failure. N Engl J Med 1996 May 30;334(22):1448-60.

(69) Thadhani R, Pascual M, Nickeleit V et al. Preliminary description of focal segmental glomerulosclerosis in patients with renovascular disease. Lancet 1996 January 27;347(8996):231-3.

(70) Thukral SK, Nordone PJ, Hu R et al. Prediction of nephrotoxicant action and identification of candidate toxicity-related biomarkers. Toxicol Pathol 2005;33(3):343-55.

(71) Toback FG. Regeneration after acute tubular necrosis. Kidney Int 1992 January;41(1):226-46.

(72) Travacio M, Maria PJ, Llesuy S. Chromium(VI) induces oxidative stress in the mouse brain. Toxicology 2000 September 7;150(1-3):137-46.

(73) Travacio M, Polo JM, Llesuy S. Chromium (VI) induces oxidative stress in the mouse brain. Toxicology 2001 May 11;162(2):139-48.

(74) Trevisan A, Troso O, Maso S. Recovery of biochemical changes induced by 1,2-dichloro propane in rat liver and kidney. Hum Exp Toxicol 1991 July;10(4):241-4.

(75) Trevisan A, Maso S. [Biological indicators of the renal involvement in workers with previous exposure to cadmium: a 5-year follow up]. Med Lav 1991 November;82(6):542-6.

(76) Trevisan A, Meneghetti P, Maso S, Troso O. In-vitro mechanisms of 1,2-dichloropropane nephrotoxicity using the renal cortical slice model. Hum Exp Toxicol 1993 March;12(2):117-21.

(77) Trevisan A, Cristofori P, Fanelli G et al. Glutamine transaminase K intranephron localization in rats determined by urinary excretion after treatment with segment-specific nephrotoxicants. Arch Toxicol 1998 July;72(8):531-5.

(78) Trevisan A, Cristofori P, Fanelli G. Glutamine synthetase activity in rat urine as sensitive marker to detect S3 segment-specific injury of proximal tubule induced by xenobiotics. Arch Toxicol 1999 June;73(4-5):255-62.

(79) Trevisan A, Giraldo M, Borella M et al. Tubular segment-specific biomarkers of nephrotoxicity in the rat. Toxicol Lett 2001 October 15;124(1-3):113-20.

(80) Trevisan A, Giraldo M, Borella M, Maso S. Historical control data on urinary and renal tissue biomarkers in naive male Wistar rats. J Appl Toxicol 2001 September;21(5):409-13.

(81) Trevisan A, Marzano C, Cristofori P et al. Synthesis of a palladium(II)-dithiocarbamate complex: biological assay and nephrotoxicity in rats. Arch Toxicol 2002 June;76(5-6):262-8.

(82) Trevisan A, Cristofori P, Beggio M et al. Segmentary effects on the renal proximal tubule due to hexachloro-1,3-butadiene in rats: biomarkers related to gender. J Appl Toxicol 2005 January;25(1):13-9.

(83) Tsou TC, Yang JL. Formation of reactive oxygen species and DNA strand breakage during interaction of chromium (III) and hydrogen peroxide in vitro: evidence for a chromium (III)-mediated Fenton-like reaction. Chem Biol Interact 1996 December 20;102(3):133-53.

(84) Tsou TC, Chen CL, Liu TY, Yang JL. Induction of 8-hydroxydeoxyguanosine in DNA by chromium(III) plus hydrogen peroxide and its prevention by scavengers. Carcinogenesis 1996 January;17(1):103-8.

(85) Turck M, Silverblatt F, Clark H, Holmes K. The role of carbenicillin in treatment of infections of the urinary tract. J Infect Dis 1970 September;122:Suppl-33.

(86) Walsh-Reitz MM, Toback FG. Phenol red inhibits growth of renal epithelial cells. Am J Physiol 1992 April;262(4 Pt 2):F687-F691.

(87) Wang XF, Xing ML, Shen Y et al. Oral administration of Cr(VI) induced oxidative stress, DNA damage and apoptotic cell death in mice. Toxicology 2006 November 10;228(1):16-23.

(88) Watanabe K, Yamada H, Yamaguchi Y. K-glypican: a novel GPI-anchored heparan sulfate proteoglycan that is highly expressed in developing brain and kidney. J Cell Biol 1995 September;130(5):1207-18.

(89) Yamaguchi K, Grant J, Noble-Jamieson G et al. Hypercalcaemia in primary oxalosis: role of increased bone resorption and effects of treatment with pamidronate. Bone 1995 January;16(1):61-7.

(90) Yamaguchi K, Tominaga T, Nishimura Y. [Clinical study on incidental renal cell carcinoma]. Hinyokika Kiyo 1995 February;41(2):93-9.

(91) Yamaguchi M, Kurota H. Expression of calcium-binding protein regucalcin mRNA in the kidney cortex of rats: the stimulation by calcium administration. Mol Cell Biochem 1995 May 10;146(1):71-7.

(92) Yamaguchi S, Jihong L, Utsunomiya M et al. [The effect of takusha and kagosou on calcium oxalate renal stones in rats]. Hinyokika Kiyo 1995 June;41(6):427-31.

(93) Yamaguchi S, Umemura S, Tamura K et al. Adenosine A1 receptor mRNA in microdissected rat nephron segments. Hypertension 1995 December;26(6 Pt 2):1181-5.

(94) Yamaguchi Y. [The structure and function of renal tubulointerstitium]. Nippon Rinsho 1995 August;53(8):1836-9.

(95) Yamaguchi Y. [The structure and function of the renal interstitial cells]. Nippon Rinsho 1995 August;53(8):1841-5.